Deliverable D4.3.3 – Innovative Concepts for Floating Structures

Partners WP4 Task 4.3
USTUTT, DTU, CENER, NTUA, RAW (only editor of report)

August, 2014

Agreement n.:	**308974**
Duration	**November 2012 – October 2017**
Co-ordinator:	**Danmarks Tekniske Universitet**
Supported by:	**FP7 – EU Programme**

The research leading to these results has received funding from the European Community's Seventh Framework Programme FP7-ENERGY-2012-1-2STAGE under grant agreement No. 308974 (INNWIND.EU).

Document information

Document Name:	Deliverable D4.3.3. – Innovative Concepts for Floating Structures
Confidentiality Class	Public
Document Number:	Deliverable D 4.3.3
Author:	USTUTT: Frank Sandner, Yu Wie, Denis Matha CENER: Enrique Grela, José Azcona, Xabier Munduate NTUA: Spyros Voutsinas DTU: Anand Natarajan
Review:	Ramboll: Tim Fischer
Date:	2014-31-08
WP:	4 Offshore Foundations and Support Structures
Task:	4.3 Structural Implementation

TABLE OF CONTENTS

(INNWIND.EU, Deliverable 4.3.3., Innovative Concepts for Floating Structures)

INTRODUCTION

This document presents the four innovative concepts for floating structures which are designed for the INNWIND.EU project by the partners DTU, USTUTT, CENER and NTUA.

The goal of the report is to indicate each design on a conceptual level and to quantify its TRL level. Based on this report, the team within WP4 will evaluate the given concepts and will decide on 1-2 concepts to be carried further within the project to a more mature level. These designs shall then also serve as basis for the second wave tank tests within WP4.

The structure of the article is the following: It gives an overview of the design assumptions which are necessary for the pre-design and then presents the innovative concepts split into four parts. At the end there is a conclusion and outlook for following steps.

DESIGN ASSUMPTIONS

Floating wind turbine support structures are a relatively young technology as compared to fixed-bottom solutions where a number of consented types have been established and successfully tested in commercial projects. Therefore the performance indicators (PIs) for the floating platform design are specifically outlined in this report. The goal is to establish a number of PIs based on a pre-design by the different partners. The PI-based assessment of innovations of the InnWind.EU project, see [1], considers mostly coupled aero-hydro-servo-elastic simulations, which are out of the scope of this report.

The design of floating offshore platforms usually starts with spreadsheet calculations for the hydrostatic properties. For specific types of platforms, e.g., semi-submersibles or spars, databases based on the extensive experience in the field of oil & gas exist. Based on these, it is relatively straightforward to preliminarily determine the overall dimensions like breadth, length and draft or the column spacing for semi-submersibles, see [2]. The initial selection of the platform type has to be based on various factors, see, e.g. [3].

For floating wind turbines (FOWT) additional requirements hold due to the aerodynamic kinetics and the rotor-dynamic forces and torques. These highly nonlinear and dynamic forces act primarily at the tower top yielding a high overturning moment and rendering the tower base section particularly critical. In addition to aerodynamic forces, the high tower top mass of the RNA yields a high gravitational overturning moment, even for a non-operating FOWT. In these respects, the loads on FOWTs differ considerably from the inertia and external loads on oil & gas platforms, for which the design driving loads are commonly a payload with a given static eccentricity and a roughly estimated wind drag. Fatigue loading is also of greater importance for FOWTs due to the high number of load cycles from the rotor dynamics. These unique aspects need to be taken into consideration when designing a floating platform for a FOWT.

This report will outline the first steps of a conceptual pre-design of a FOWT platform and the corresponding PIs. A rough overview of the FOWT design process is given by the following list.

1. Selection of platform type (ballast, buoyancy, mooring stabilized) based on the list of requirements.

2. Hydrostatic analyses giving the design space with appropriate hydrostatic properties. The relevant structural quantities like mass, center of mass and moment of inertia can be formulated.

3. Material and manufacturing cost estimates for all possible designs gives an approximate CAPEX and assesses the design feasibility.

4. Potential flow solvers with a preliminary conceptual mooring system allow dynamic simulations assuming a rigid floating body (manoeuvring/seakeeping analysis). The dynamic behaviour is optimized for intransient situations.

5. Improved mooring system design for an appropriate added stiffness, static load on the fairleads and steady-state excursions of the platform.

6. Coupled dynamic analysis with aero-servo-hydro-elastic software tool show the dynamics in realistic conditions and outline critical cases, see design load cases (DLC) of [1].

7. Experimental wave tank tests approve numeric simulations and outline critical cases. Hydrodynamic coefficients are tuned.

8. Critical load case review with advanced software tools (nonlinear waves, drift forces, green water, etc.).

9. Detailed LCOE estimation, including CAPEX and OPEX, complete design and site data, see [4].

10. Detailed component design including structural dimensioning based on coupled simulations according to offshore standards.

11. Determination of the manufacturing and installation process, maintenance, logistics, health and safety, environmental and legislation aspects.

The design process is naturally an iterative process, which means that the steps will have to be repeated several times. Product design guidelines like [5] might be helpful. Comparable studies specific to FOWT can be found in the literature, e.g., for a semi-submersible FOWT [6], [7] and [8], a spar FOWT [9] and [10] and a TLP FOWT [11] and [12]. The design process for offshore structures is outlined in [2], p.428.

This report addresses the pre-design of different concepts and their comparison which includes the first four points of the list above.

Environmental Conditions

A concept of a floating wind turbine should usually be adapted to the site it is designed for. The InnWind 10MW reference turbine [13] has been designed for Class 1b and a shallow-water site of 20m depth, see [14]. For the first design load calculations which are commonly a selection of IEC 61400-3 design load cases (DLC). The combination of the peak spectral period T_p and the significant wave height H_s and its correlation to the wind speed for normal and extreme conditions (recurrence periods of $1 - 50a$) is required, as well as information on directionality (wind/wave misalignment and wave spreading). For the Innwind.EU project, the wind-wave conditions have to be assumed for this design since there is no site data available for a deep-water site in the project so far. The *water depth* for D4.3.2 is assumed to be 200m as in the OC4 study, [15].

Hydrostatics & Stability

In O&G industry, the floating behaviour shall be consistent with the requirements for stability in all conditions including intact and damaged configurations, for both temporary and in-service conditions. The stability (righting stability) requirements are typically analysed according to ISO-19901-6. As an alternative the dynamic-response-based intact stability criteria incorporating the dynamic motion response characteristics is used, as e.g. outlined in the IMO Intact stability code.

Key

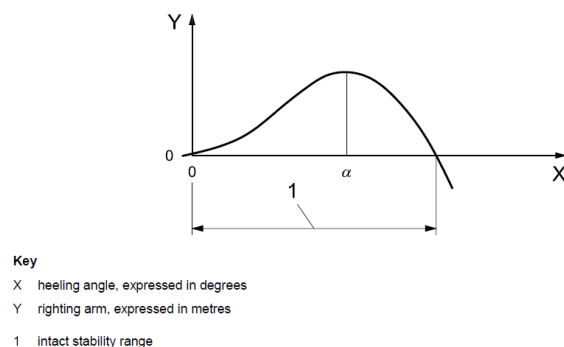X   heeling angle, expressed in degrees

Y   righting arm, expressed in metres

1   intact stability range

Figure 0.1 – Illustration of stability terms according to ISO 19901-6

(INNWIND.EU, Deliverable 4.3.3., Innovative Concepts for Floating Structures)

For FOWT the hydrostatic restoring is particularly important (independent of the site conditions) due to the aerodynamic thrust force and its direct implication on the annual energy production which decreases approximately by the cosine of the resulting mean platform tilt. Most important is the rotational restoring stiffness about the axis perpendicular to the wind direction (y), see the sketch in Figure 0.2. Looking at first at the steady-state behaviour of the system, the hydrostatic restoring stiffness C_{55} determines the vertical wind misalignment dependent on the thrust force magnitude due to the pitching of the floater. In the field of offshore engineering the metacentric height M is often used for stability assessment. However, this does not take into account the mass of the system and does therefore not yield a value for the restoring stiffness. Regarding the dynamic behaviour the still-water eigenperiod in the same rotational direction (55) of the system is not only determined by the stiffness C_{55} but also by the system inertia I_{22}. According to [2] the wave excitation resonance (RAO) in all degrees of freedom (DOF) shall lie always above $T_{eig,min} = 25\ s$, which is above most common wave spectra.
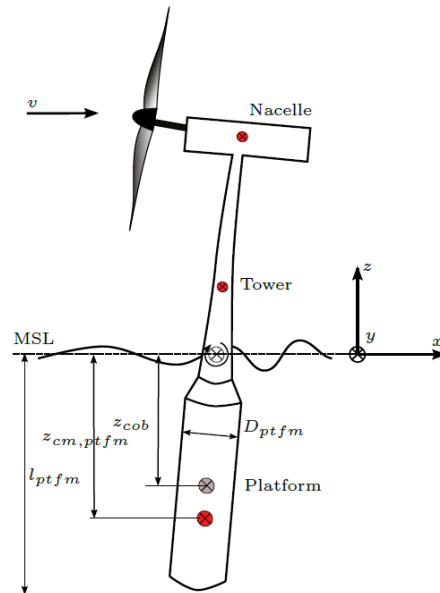

Figure 0.2 – FOWT system topology

The linearized hydrostatic restoring stiffness of the whole FOWT system about y about the sea water level (SWL) with various bodies i with their center of mass located at z_i above SWL, see Figure 0.3, can be calculated as

$$C_{55} = \sum -z_i m_i g + M_{wtrpln} + z_{COB} m_{FOWT} g + C_{Lines}. \qquad (1)$$

The waterplane area yields a restoring, which can be calculated using the second moment of area of the horizontal cross-section at SWL, see [16]. The influence of the buoyancy is destabilizing since $z_{COB} < 0$. The restoring from the mooring system C_{Lines} is mostly important for tension-leg platforms (TLP), where the other components of Equation (1) do not suffice to ensure stability of the FOWT. See [11] for a TLP conceptual design process. For all other platform types the mooring system introduces a quite small portion to the restoring and can therefore be dimensioned in subsequent design steps.

(INNWIND.EU, Deliverable 4.3.3., Innovative Concepts for Floating Structures)

The hydrostatic restoring stiffness C_{55} has been determined for InnWind task 4.3 as to yield the same pitch angle under steady rated wind conditions as the OC4 system, [15]. This steady state pitch angle is $\beta_{rated} = 3.5 \deg$ for a rated thrust force of $F_{thrst,rated} = 1.5 \times 10^6$ N. It is recommended in this report to start the platform design process with a fixed hydrostatic restoring stiffness as the first requirement that defines the design space for all further optimization. The value for the hydrostatic restoring C_{55} according to equation (1) is

$$C_{55,InnWind} = 2.922E9 \text{ Nm/rad.} \tag{2}$$

In further design steps the nonlinear hydrostatic restoring can be computed in order to assess the restoring properties for larger pitch angles, see [17]. Applied to a spar-type platform, for example, the platform draft over its radius for a constant C_{55} can be computed, see Figure 0.4.

Going back to the steady-state characteristics it is mentioned that the steady-state pitch-angle of the platform can be also influenced by a slow actuator-system like interconnected water tanks (active ballasting concept used by PPI's WindFloat semi-sub, see [18]). Thus, this shifting of ballast within the platform can reduce the wind misalignment of the rotor.
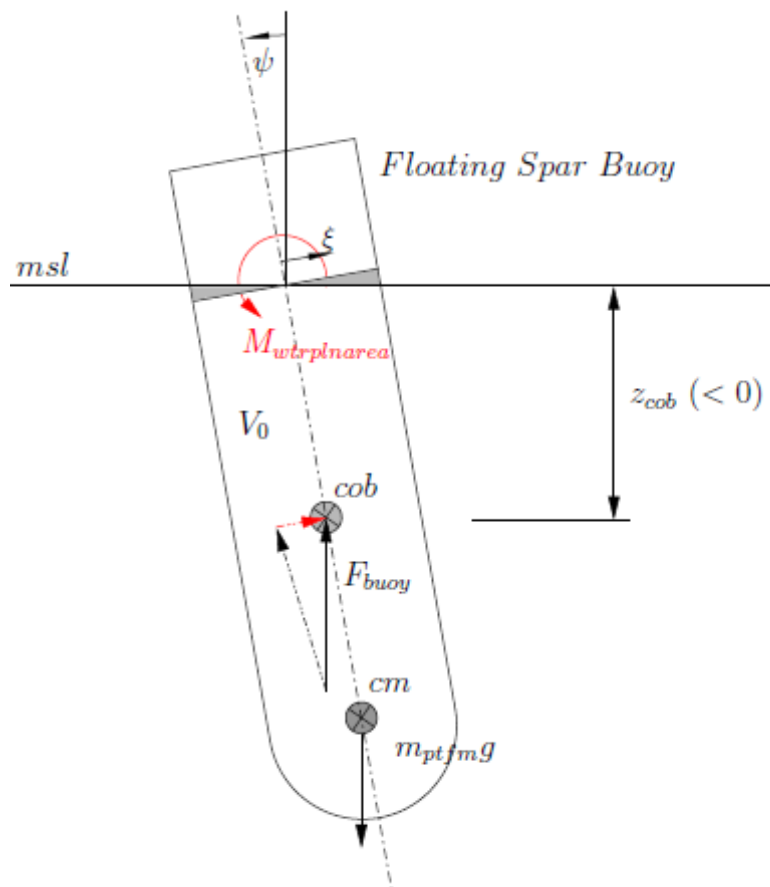

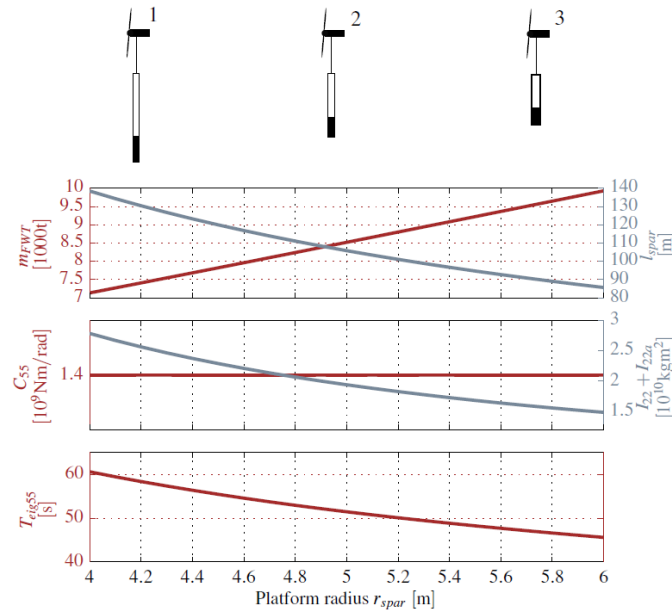Figure 0.3 – Hydrostatic forces on a floating body

(INNWIND.EU, Deliverable 4.3.3., Innovative Concepts for Floating Structures)

Figure 0.4 – Spar design space for $C_{55} = const$

Still-water Eigenperiod

When estimating the additional mass moment of inertia from the added mass, $I_{22,a}$ the still-water eigenperiod can be estimated as done in [5] as

$$T_{eig,55} \approx 2\pi \sqrt{\frac{C_{55}}{I_{22} + I_{22,a}}}. \tag{3}$$

It is possibly relevant to consider different reference points when calculating Equation (3) depending on the prevailing center of rotation of the FOWT. A good guess might be the overall system center of mass, or as proposed in [19], the center of buoyancy (COB).

To some extent the still water eigenperiod is correlated with the RAO peak frequency so that even before numerical computations are performed this information on the dynamic behaviour is available. For platform types with an eigenperiod $5\,s < T_{eig,55} < 20\,s$ close to common wave spectra this can be an early exclusion criterion.

Typical ranges for the design eigenperiod values for offshore structures in general are $T_{eig,33,max} > 20\,s$ for semi-submersibles, and for spars the maximum heave period $T_{eig,33,max}$ should be higher than two times the peak storm wave period, see [2].

Seakeeping and Manoeuvring

Once all suitable platform geometries (and according mooring systems for TLPs) have been derived based on hydrostatic requirements the further selection is done based on the calculation of hydrodynamic panel codes, like [20] or [21]. These potential flow solvers usually separate the fluid-structure interaction problem into the seakeeping (or diffraction) and the manoeuvring (or radiation) problem. These are solved in frequency

(INNWIND.EU, Deliverable 4.3.3., Innovative Concepts for Floating Structures)

domain for regular waves. The coupled problem returns the previously mentioned wave resonance operators (RAO). The separate solution of the manoeuvring problem gives the added mass A $(n_{frq}\times 6)$ and radiation damping B $(n_{frq}\times 6)$ for the sinusoidally oscillating platform. The separate solution of the seakeeping problem gives the frequency-dependent wave excitation vector X $(n_{frq}\times n_{wavedir}\times 6)$.

The frequency-domain solution to both problems allows selecting platforms with a low off-peak RAO and a peak frequency off the considered wave spectrum. The solution to the seakeeping problem gives the peak wave excitation force and frequency only dependent on the hull shape. The manoeuvring problem gives the additional mass and damping properties which can be augmented to the mass properties of the platform. Thus, these properties can be written as part of the structural system equations of motion, see [22]. Since the manoeuvring problem assumes zero wave kinematics the added mass and damping allow the calculation of the still-water eigenperiod.

Consequently, a differing peak wave excitation frequency and still-water eigenfrequency, both off the peak spectral wave frequency is targeted. The radiation, diffraction and added mass dynamic properties are influenced by the platform geometry only. If the designer does not want to alter the general geometry additional hydrodynamic features can be used to improve the design. For the adjustment of the added mass properties heave plates are a common option, see [18].

Finally, the damping of the system is a value that is hard to estimate at this design stage. However, it is possible to classify floating offshore platforms according to the prevailing type of hydrodynamic forces exerted on them. Dependent on the significant dimensions of the platform and the wave kinematics either viscous or diffraction effects are of importance, see [23].

Mooring System

Except for TLPs the mooring system dynamics can be excluded for this design stage. When looking at the coupled dynamic behaviour, it is advisable to represent the mooring lines with a linear spring stiffness acting on the overall center of mass of the system, see [22]. The adjustment of the restoring characteristics in all directions (diagonal and off-diagonal) can be a convenient parameter for system optimization in further design stages. In the later design stages, the mooring system needs to be designed according to e.g. ISO 19901-7, and for TLPs according to recognized industry standards, such as API.

InnWind 10MW Reference Wind Turbine

The reference wind turbine used for the design of the InnWind innovative floating platform can be found in deliverable D1.2, the description of the InnWind 10MW reference wind turbine, see [13].In order to adjust the wind turbine geometry for the use on a floating platform, the interface between platform and tower has been defined at the height h_{twrbs} above SWL

$$h_{twrbs} = 12 \text{ m.} \tag{4}$$

Thus, the tower has been cut off, omitting the first 12 m and keeping the upper 103.63 m in order to maintain the hub height of 119 m (including the offset between tower top and center of the hub).

For the potential flow calculations and mainly the 6×6 mass matrix of the wind turbine is important for the calculation of the RAOs. It has been calculated with the new tower definition taking the SWL as a reference as

(INNWIND.EU, Deliverable 4.3.3., Innovative Concepts for Floating Structures)

$$M_{10MW} =$$

$$
\begin{bmatrix}
1.144E+06 & 0 & 0 & 0 & 9.547E+07 & -1.250E-01 \\
0 & 1.144E+06 & 0 & -9.547E+07 & 0 & -5.948E+05 \\
0 & 0 & 1.144E+06 & 0 & 5.948E+05 & 0 \\
0 & -9.547E+07 & 0 & 9.299E+09 & 0 & 5.814E+07 \\
9.547E+07 & 0 & 5.948E+05 & 0 & 9.239E+09 & -1.450E+01 \\
0 & -5.948E+05 & 0 & 5.814E+07 & -1.450E+01 & 9.997E+07
\end{bmatrix}.
$$
(5)

Coupled System Considerations

Once a generally suitable range of platform geometries has been found the coupled system has to be analysed. This is important due to various coupling effects, which are not identifiable when looking at the separated subsystems, e.g. interactions of hydrodynamics, structural dynamics or aerodynamics. For tower vibrations the Campbell diagram is a useful means for avoiding resonances from the rotor rotation, see [24]. When the platform is connected to the wind turbine also platform resonances can shift, see [25], depending on the relation between the frequency of external force and the natural frequency of structural vibration (platform concept dependent). A wind misalignment can yield yaw-excitations which require a thorough adjustment of the restoring stiffness of the mooring system in yaw direction. Simplified numerical models are very useful at this design stage. See, e.g., [26], [27] and [28].

Material Cost Estimation

For comparing different design solutions after the first conceptual dimensioning the material cost is an important quantity. Assuming a hull steel cost of 3000 €/t, a hull material cost of reinforced concrete of 250 €/t and a ballast material cost of 70 €/t the overall material cost of the platform can be calculated. These values depend, of course, also on other parameters, like the complexity of the structure and therefore the amount of welding, which should also be taken into account. Although detailed structural calculations are excluded in the conceptual pre-design realistic wall thicknesses and reinforcements have to be taken into account.

Installation Process

Depending on the platform type the installation process can take a large portion of the CAPEX. For a TLP the preparation of the soil and fixation of the anchors as well as the mooring lines are expensive. It is further necessary to determine early in the design process where which parts of the platform are built and how the transportation and assembly of the system can be done. At many sites the sea depth around the harbors and construction sites can be a hard limitation.

Conceptual Design Performance Assessment and Comparison (KPIs)

For a comparison of the conceptual designs the parameters of Table 0.1 are selected for an initial comparison. Additionally, it is useful to characterize the hydrodynamic forces on the designed platform in terms of whether they are dominated by viscous forces or diffraction forces, see [23].

Table 0.1 – Conceptual Design Parameters

Value	Symbol	Unit
System mass	m_{FOWT}	kg
Basic dimensions: breadth, length, draft, diamter	b, w, d, D	m
Hydrostatic Stiffness about y at SWL for the entire FOWT (list contributions from gravity, buoyancy and waterplane area)	C_{55}	Nm/rad
RAO	$RAO(f, 33, 55)$	[-]
Wave excitation force per total system mass	$\frac{X_{11}(f)}{\mathrm{m_{tot}}}, \frac{X_{55}(f)}{I_{22,tot}}$	N/kg ; Nm/(kgm²)
Still water eigenperiod	$T_{eig,33}, T_{eig,55}$	s
Material cost	C_{mat}	€

(INNWIND.EU, Deliverable 4.3.3., Innovative Concepts for Floating Structures)

STRUCTURAL CONCEPTS

In the next four chapters the innovative concepts for floating structures of offshore wind turbines are presented. The pre-designs are developed by the four partners, DTU, USTUTT, CENER and NTUA. Following a short introduction into each design concept, the design results are specified, advantages and disadvantages are discussed and summarised in a conceptual conclusion.

The first semi-floater concept is designed by DTU. It is a new floating platform that is constrained to the sea floor through an articulated joint and a mooring system.

The second concept is invented by the USTUTT and predominantly made out of concrete. The proposed shape of the floating platform can be classified as a spar with modifications to allow a reduction of the overall draft.

The third and fourth part of this report present two modifications of semi-sub floater concepts, pre-design by CENER and NTUA.

The platform of the CENER design basically consists on an equilateral triangle with three stabilizing columns, one in each vertex joined by three pontoons. The wind turbine is located in one of the columns, to avoid the use of an additional central column.

The conceptual design investigation carried out at NTUA aimed at considering different variants that ensure suitability in a wide range of depths.

The basic element in the conducted investigation is a cylindrical torus with or without heave plates which was considered either in combination with a spar buoy or as the only buoyancy delivering element.

PART I: SEMI-FLOATER CONCEPT (DTU)

Introduction

A new floating platform that is constrained to the sea floor through an articulated joint has been design for water depths of 50 m for the 10MW DTU reference wind turbine (RWT). The goal of this new design is to look for a cheaper alternative for 50+ m water depth than the traditional jacket structure. The new platform is strongly anchored to the seabed with a spherical joint which constrains all translation, but allows rotation. The system presented in this report includes a mooring system, a laminated rubber articulated joint and a floater composed by two different bodies: a steel cylinder and a buoyancy chamber.

The performance of the system and the conclusions thereof is discussed herein.

Design concept

The 10MW reference wind turbine is mounted on a spar-buoy type platform that is anchored to the soil using an articulated join that is free to rotate, but constrained from translation. The platform has a composite material buoyancy chamber near the sea surface and concrete ballast near the soil. The dimensions of the sub structure are provided in Figure I.1

(INNWIND.EU, Deliverable 4.3.3., Innovative Concepts for Floating Structures)
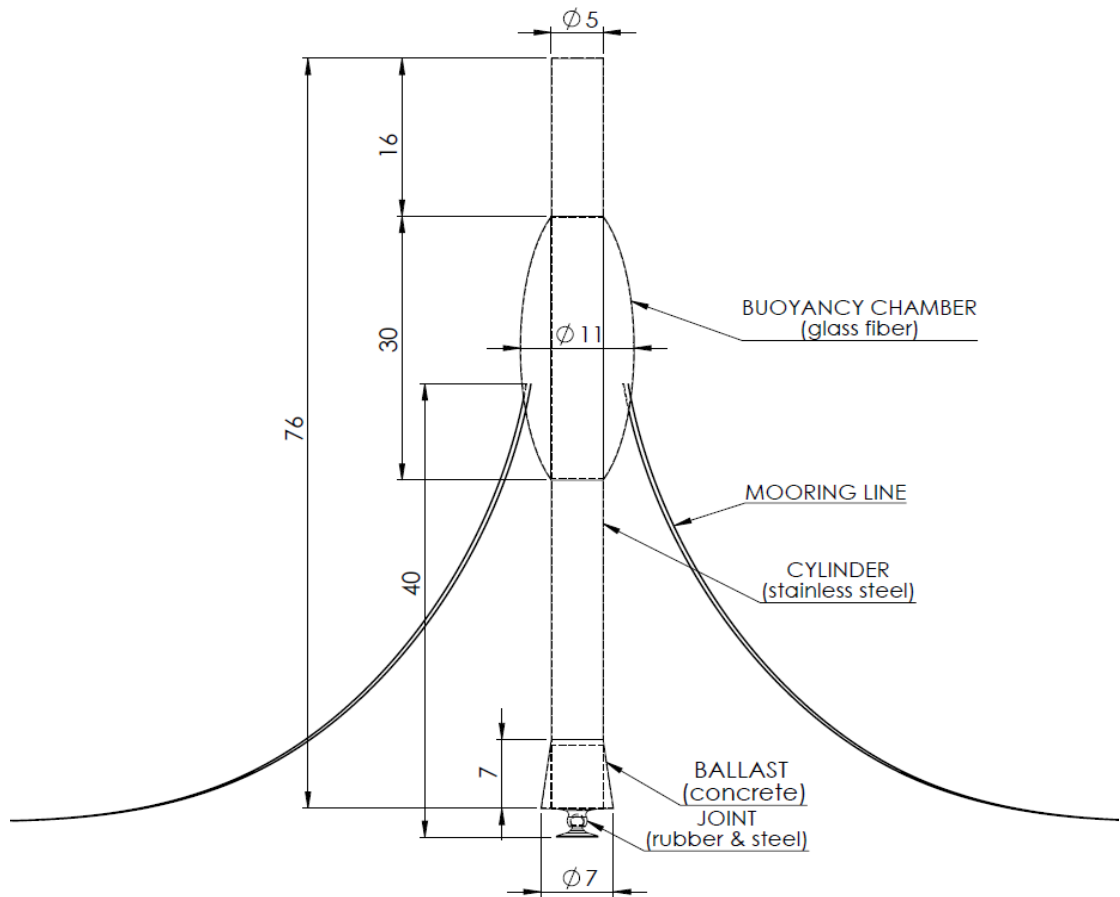
Figure I.1 – Geometry of the semi floater sub structure for the 10MW reference wind turbine

All the components parts are depicted in Figure I.1 and are described in detail in the deliverable report D4.12 [29] and hence not repeated here.

Design Results

A multi body model of the floater system was developed and the characteristic performance curves of the 10MW system (aerodynamic power, rotational speed of the rotor, thrust force at the rotor, pitch angle of the blades and pitch angle of the platform) are obtained by simulating the complete wind turbine system in the HAWC2 aeroelastic software [30]. Class 1 A wind conditions are assumed. A controller similar to the NREL 5MW floating turbine control system [31] for suppressing the pitch system instability was implemented. The steady state curves are obtained through a slow wind ramp from cut-in to cut-out. Diverse performance parameters were measured. It should be noted that for this simulation the waves used were for a constant significant wave height corresponding to a normal sea state. The steady state results are depicted in Figure I.2 to Figure I.5.
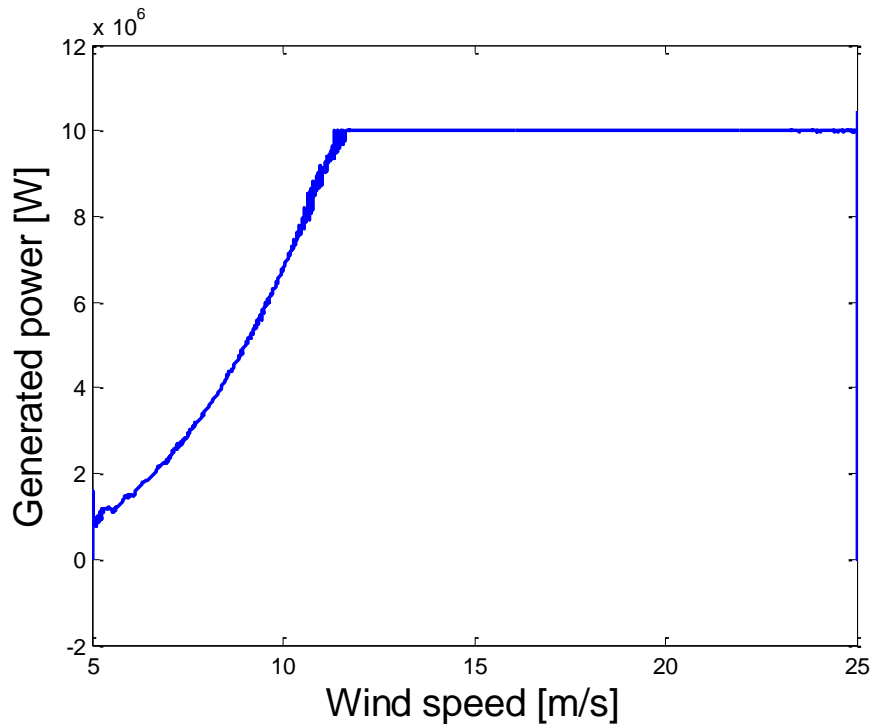
(INNWIND.EU, Deliverable 4.3.3., Innovative Concepts for Floating Structures)

Figure I.2 – Simulated Steady power curve

Figure I.3 – Thrust force curve
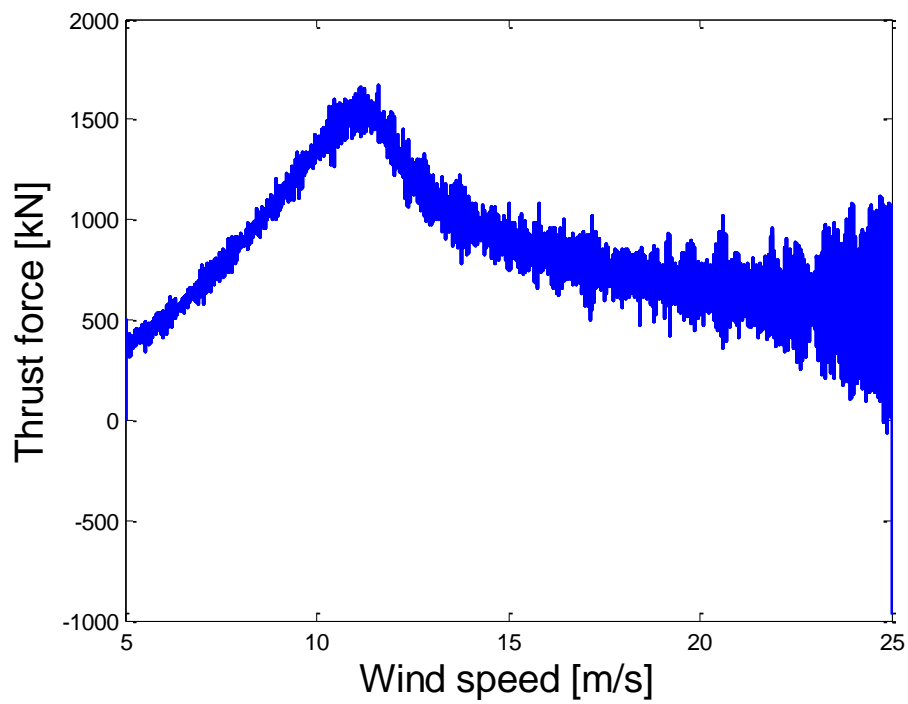
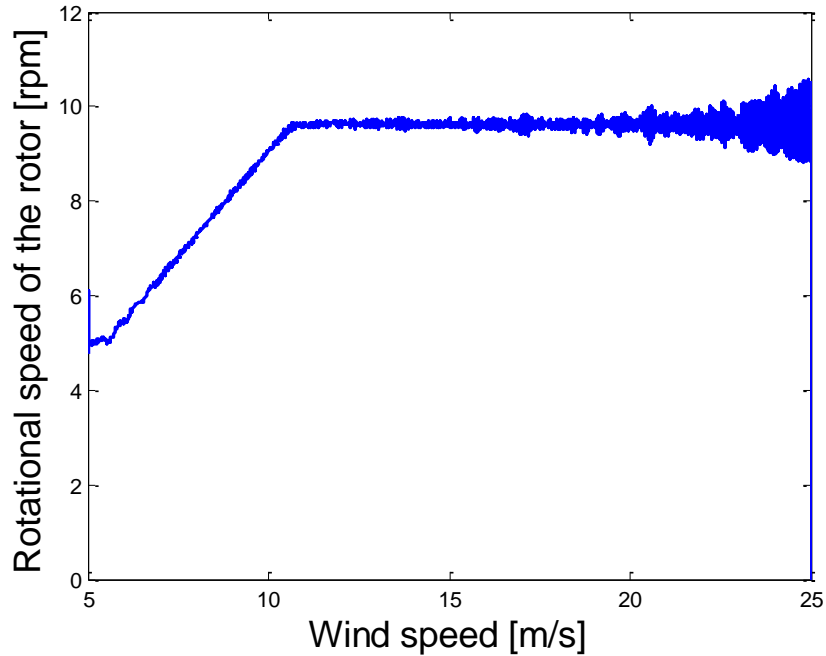*(INNWIND.EU, Deliverable 4.3.3., Innovative Concepts for Floating Structures)*

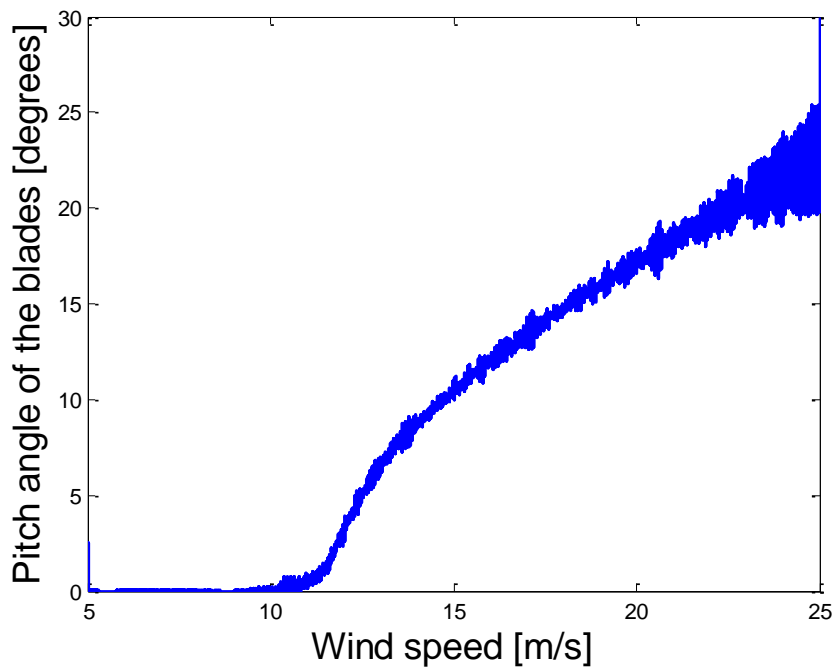Figure I.4 – Rotational speed curve of the rotor

Figure I.5 – Pitch angle of the blades

The values obtained in Figure I.2 to Figure I.5 show that the power curve of the 10MW turbine is maintained and that at high mean wind speeds, there is some oscillations of the thrust force due to the pitching of the platform. The influence of the significant wave height has been found minimal in these results.

(INNWIND.EU, Deliverable 4.3.3., Innovative Concepts for Floating Structures)

Fully coupled aero-servo-hydro-elastic load simulations for understanding the fatigue on the support structure, extreme loads and the stability of the floater are simulated in HAWC2 to verify the system integrity. The main load cases that are run are DLC 1.1/1.2 with normal sea states and normal turbulence with yaw misalignments of +/- 10 degs and DLC 6.2, that is the 50 year storm with loss of electrical connection. The following sections   provide   the   results   of   the   load   case   simulations.

DLC 1.1 – NORMAL wind turbulence/power production (NTM)

This DLC includes mean wind speeds in the normal operational range (from 5 to 25 m/s) of the wind turbine. The waves are aligned with the main direction of the wind. For one third of the simulations there is no yaw error; the rest of the simulations have a yaw error of ±10°. For each mean wind speed, 6 different seeds of wind turbulence have been simulated. The significant wave height at each mean wind speed is given in Table I.1.

Table I.1 – Significant wave height and wave period depending on the wind speed

Ws [m/s]	Hs [m]	Tp [s]
5	1.286	4.490
7	1.857	5.397
9	2.429	6.171
11	3.000	6.859
13	3.571	7.484
15	4.143	8.060
17	4.714	8.598
19	5.286	9.104
21	5.857	9.584
23	6.429	10.040
25	7	10.477

The load values analyzed at this section have been: Damage equivalent forces and moments at the tower-top in the three main directions (x, y and z) and the pitch angle of the platform. The blue lines represents the results from the simulations with no yaw misalignment error; the red data shows the results from the simulations where the wind has a -10° misalignment error; the green curves show the results from the analysis of the simulations with a +10° yaw misalignment error.

(INNWIND.EU, Deliverable 4.3.3., Innovative Concepts for Floating Structures)
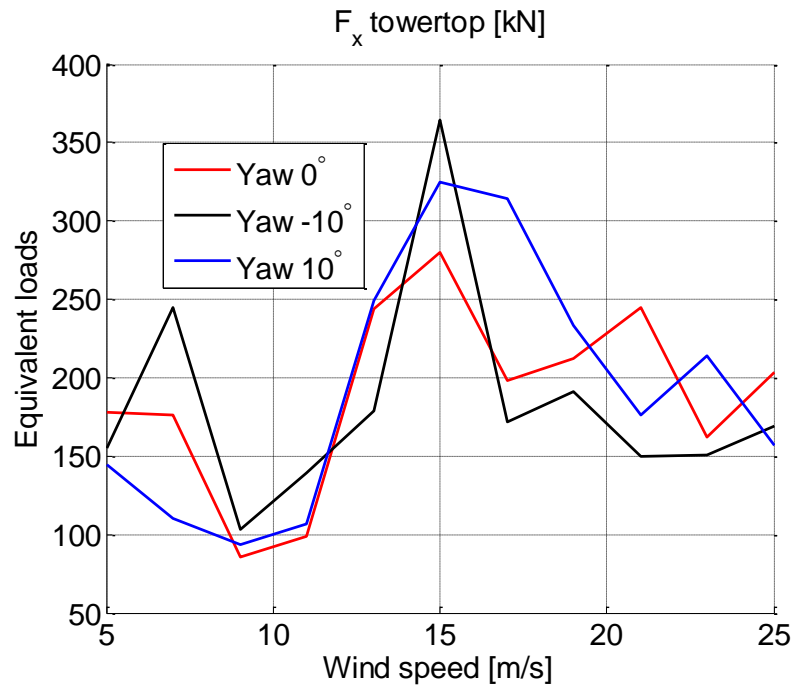
Figure I.6 – Equivalent Tower top Side Side fatigue force for the lifetime of the turbine

Figure I.7 – Statistical values of the tower top side-side force

(INNWIND.EU, Deliverable 4.3.3., Innovative Concepts for Floating Structures)
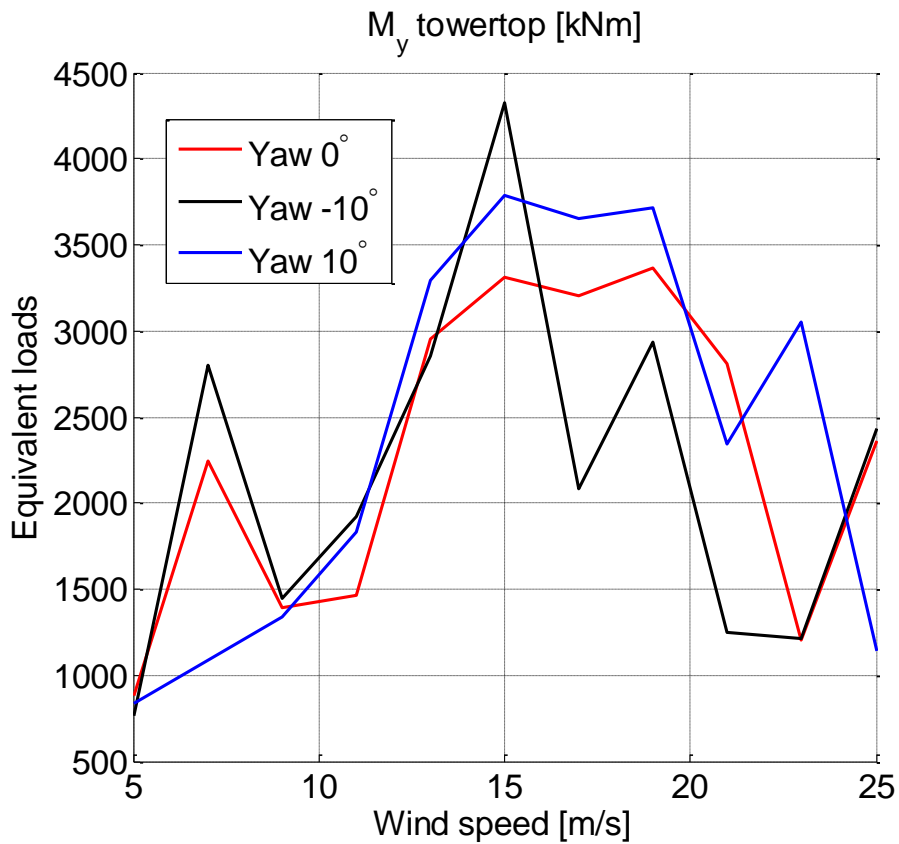
Figure I.8 – Equivalent Tower Top side-side fatigue moment for the lifetime of the turbine

Figure I.9 – Statistical values of the Tower Top side-side fatigue moment

(INNWIND.EU, Deliverable 4.3.3., Innovative Concepts for Floating Structures)

In Figure I.6 and Figure I.7 it is noticeable that the values of the equivalent fatigue loads for force at the tower top in the side-side direction are quite low. The reason for this is that the mean value is close to zero and the standard deviation is relatively small except at values close to the rated wind speed (as it was expectable because the mooring lines should balance their forces with each other, see Figure I.13). This behavior affects the corresponding moment in the Y direction at the tower top.

In Figure I.10 -Figure I.14 the damage equivalent loads of the tower top thrust are plotted which show bounded magnitudes that suggest the thrust load is well controlled by the pitch controller without any instabilities. It can also be seen that the mean values of the thrust force at the tower top are small and they follow the trend of the thrust force curve for the lowest values of wind speed (at low wind speeds the wave forces are also lower and they have a smaller influence than at higher wind speeds). The low values of this mean show very good balance between the different mooring lines. They manage to distribute in an efficient way the reaction forces to the thrust and wave forces at the tower top and balance those forces between the different mooring lines.

The same behavior can be observed in Figure I.12 and Figure I.13 for the thrust moment at the tower top.
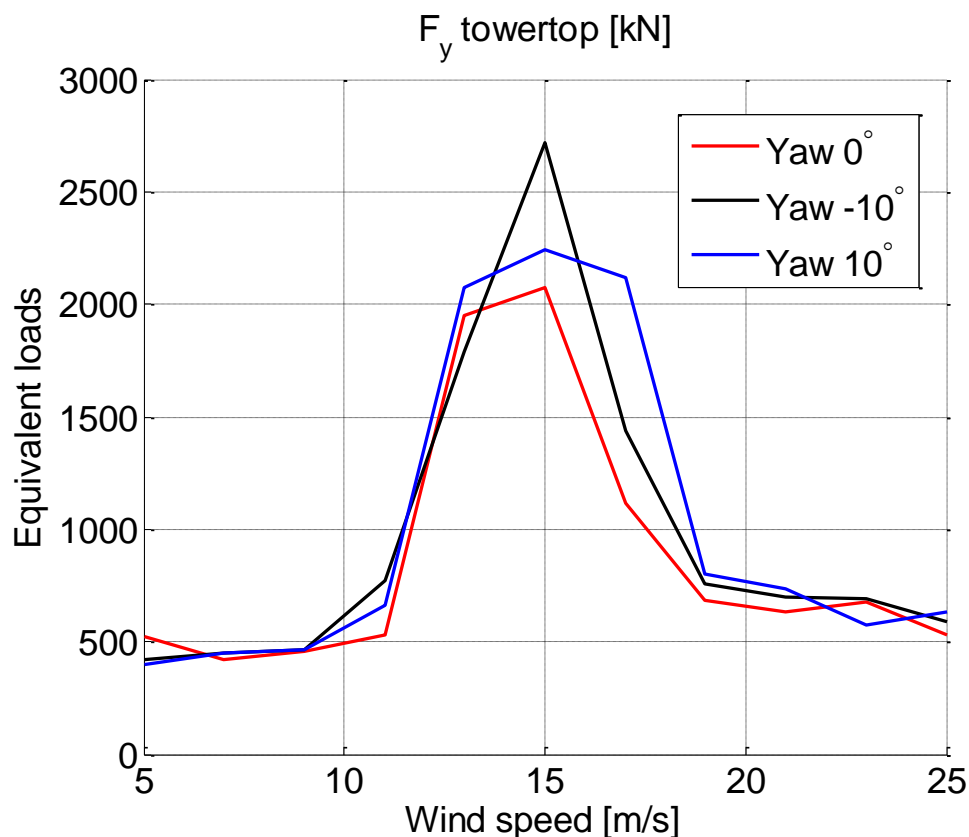

Figure I.10 – Equivalent fatigue loads for the tower top thrust force

(INNWIND.EU, Deliverable 4.3.3., Innovative Concepts for Floating Structures)
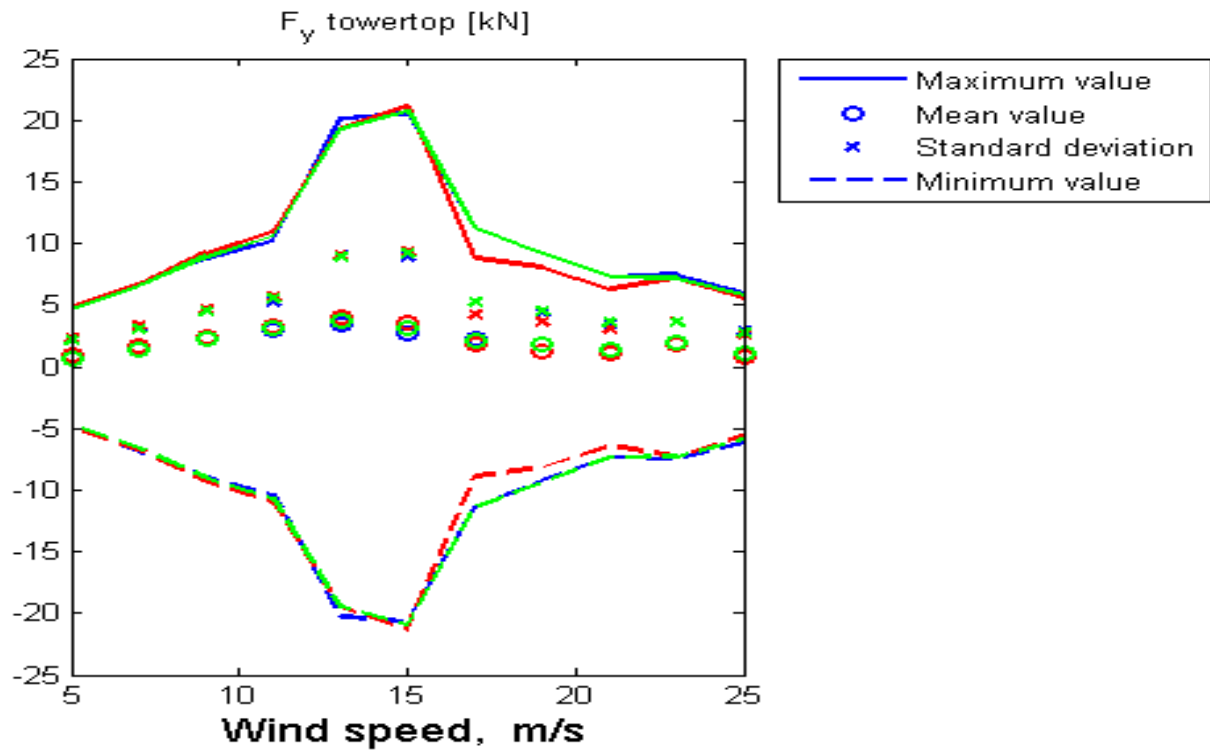
Figure I.11 – Statistical values of the thrust force at the tower top

Figure I.12 – Equivalent fatigue loads for the tower top moment in the thrust direction

(INNWIND.EU, Deliverable 4.3.3., Innovative Concepts for Floating Structures)
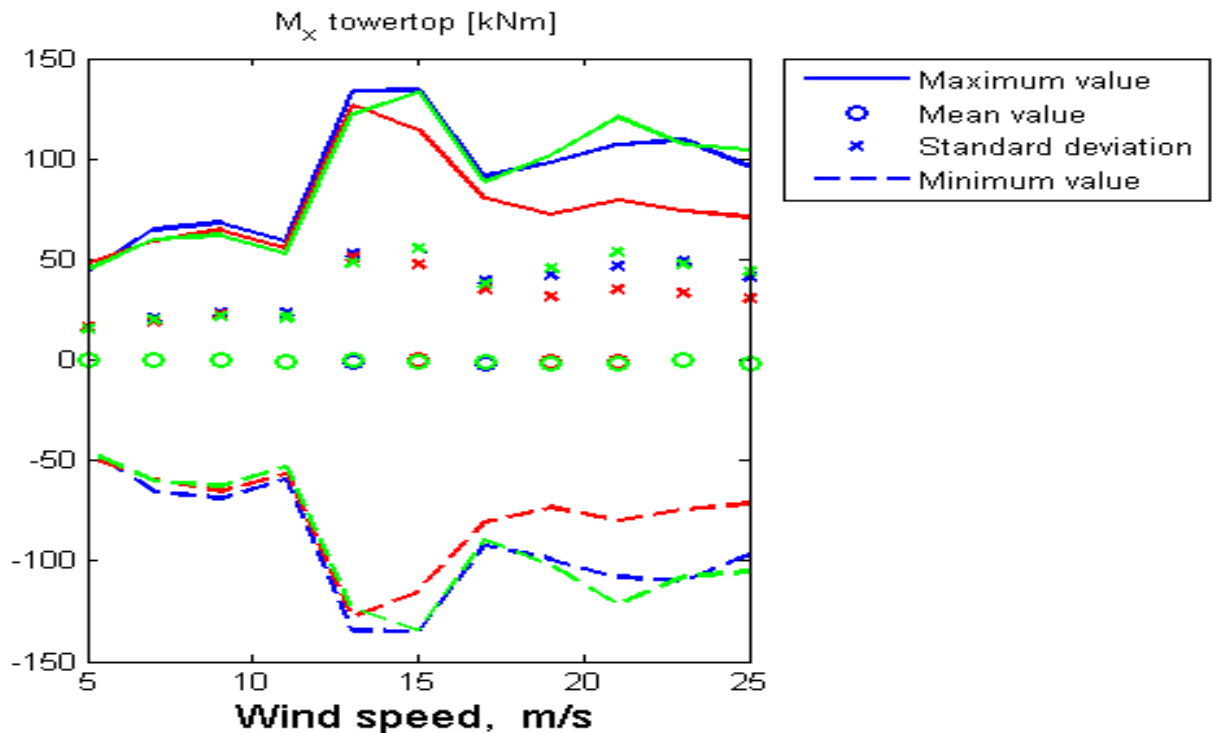
Figure I.13 – Statistical values of the tower top moment in the thrust direction.

For the case of the vertical force at the tower top, the averaged value is quite constant for all wind speeds (this is the weight of the nacelle). This is reasonable because the main forces acting vertically are the weight and the buoyancy force. The buoyancy force depends on the wind speed indirectly: the buoyancy force depends on the submerged volume of the floater, and this is a function of the pitch angle of the platform. At the same time, the pitch angle of the platform depends on both the wave forces and the wind speed (and the thrust force that is generated). As the wind and wave induced forces increase, it is necessary to submerge more volume in order to obtain enough restoring moment for reaching the equilibrium.

The mean platform pitch angle as observed in Figure I.14 shows that the pitch controller maintains a near 0 deg. mean angle until rated wind speed, beyond which the platform pitch angle increases till its maximum value at a mean wind speed close to 15 m/s. A different trend depending on the yaw misalignment angle is shown and the largest angles are observed when the angle of the yaw misalignment is negative.
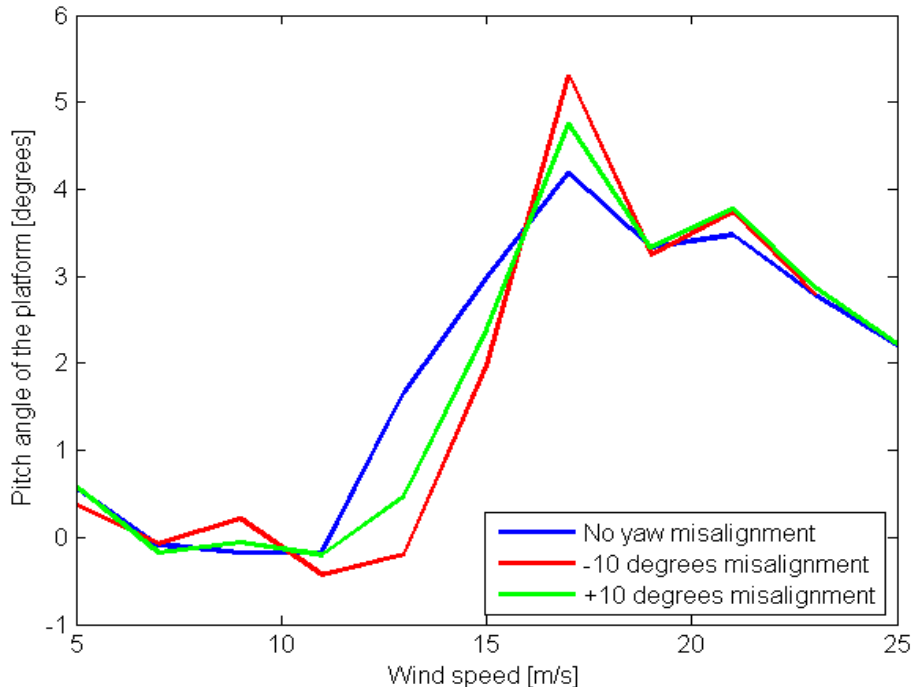
Figure I.14 – Averaged values of the platform pitch angle.

DLC 6.2 – STORM CASE

This DLC is simulated using a mean wind speed of 50 m/s coming from different directions (0°, 30°, 60°, 90°, 120°, 150°, 180°, 210°, 240°, 270°, 300° and 330°) with the turbine in an idling condition.

In this DLC, the external loads on the system from the waves are significant. The wind induced forces are also high but as the blades are pitched to 90°, the influence of the thrust force on the floater is minimized. The waves used for this DLC have a significant wave height of 12 m and a peak spectral period of 13.7 s. The JONSWAP spectrum is used to simulate the irregular waves.

The main objective of the study is to quantify the magnitude of the extreme loads on the joint at the sea floor and to demonstrate that the platform is stable even when the turbine is not operational and subject to extreme wind and waves.

The waves are misaligned with the wind direction in the sense that the wind directions are changed, keeping the wave direction the same. For each wind direction, 6 different wind and wave seeds have been simulated. The maximum and minimum values of the characteristic load at each of the studied channels have been considered..

In Figure I.15, it can be seen that the side-side loads reach their maximum when the wind is coming from 90° and 270° with respect to the rotor. The sign of the extreme force depends on the direction of the incoming wind.
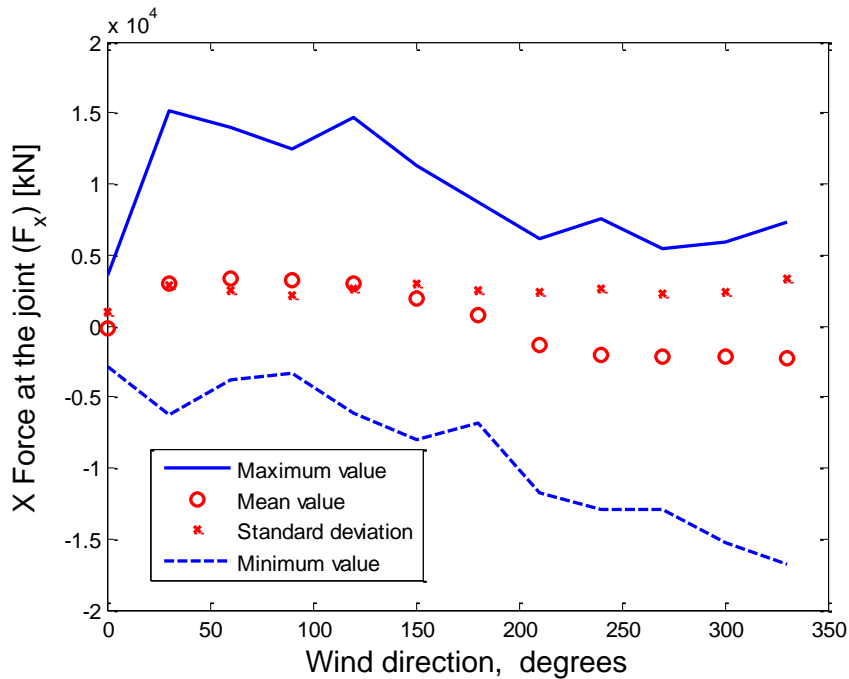
Figure I.15 – Force in side-side direction at the joint on the sea floor

The joint loads in the fore-aft direction are dominated by the waves for all the cases. As the wave direction is constant, we can see that there is not a wide variation in loads with wind direction. In Figure I.16, the mean load value and the standard deviation is near constant. In the cases when the wind direction is aligned with the waves (reverse and same direction) the results differ based on the phase angle of wind and waves.
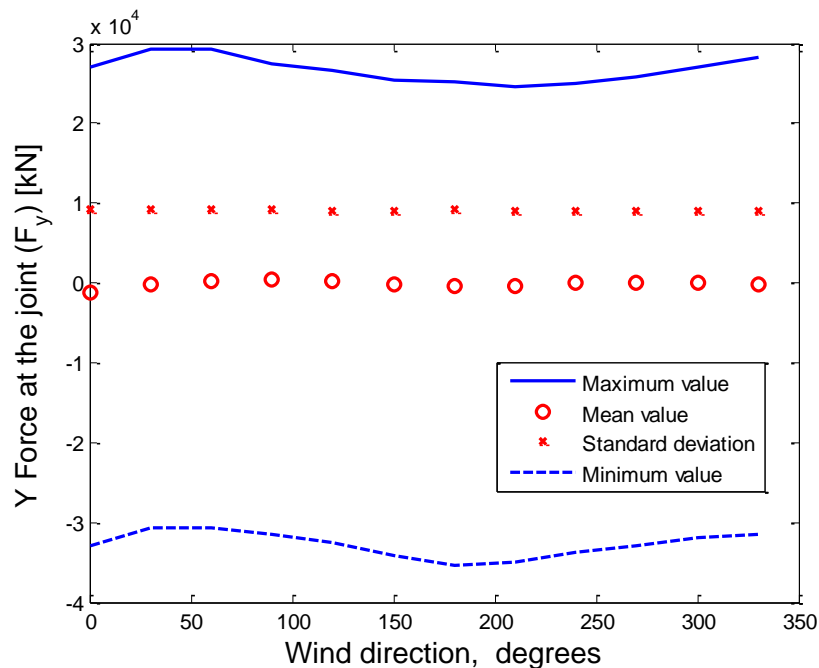

Figure I.16 – Force in Fore-Aft direction at the joint.

(INNWIND.EU, Deliverable 4.3.3., Innovative Concepts for Floating Structures)

In the case of the vertical forces (Figure I.16) the extreme values obtained are mainly constant for all the scenarios, which is expected. The values obtained for the vertical force at the joint in this load case (DLC 6.2), are smaller than the ones obtained for the previous load case (DLC 1.1). The main cause of this is that the bigger waves load the system with both positive and negative loads; while during normal operation the system only gets negative loads (the buoyancy is higher than the weight).

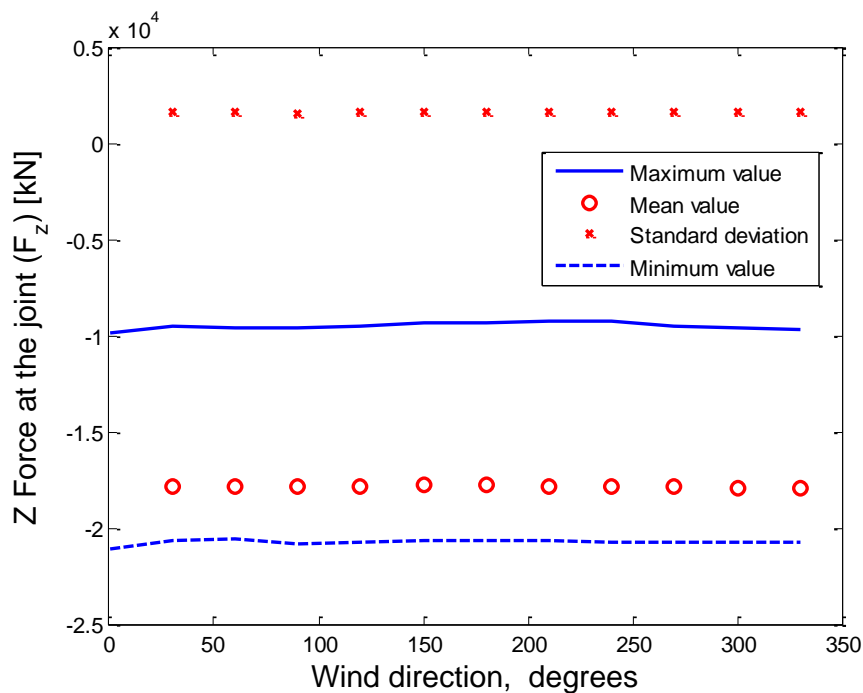Figure I.17 – Force in Z direction at the joint.

In Figure I.18, the pitch angle of the platform is displayed and it can be observed that the values for the pitch angle of the platform are bounded between -4 degrees to 8 degrees. The biggest angle is obtained at 0 degree wind direction which is direct towards the rotor, which may be expected due to the alignment of the wave and wind induced loads.
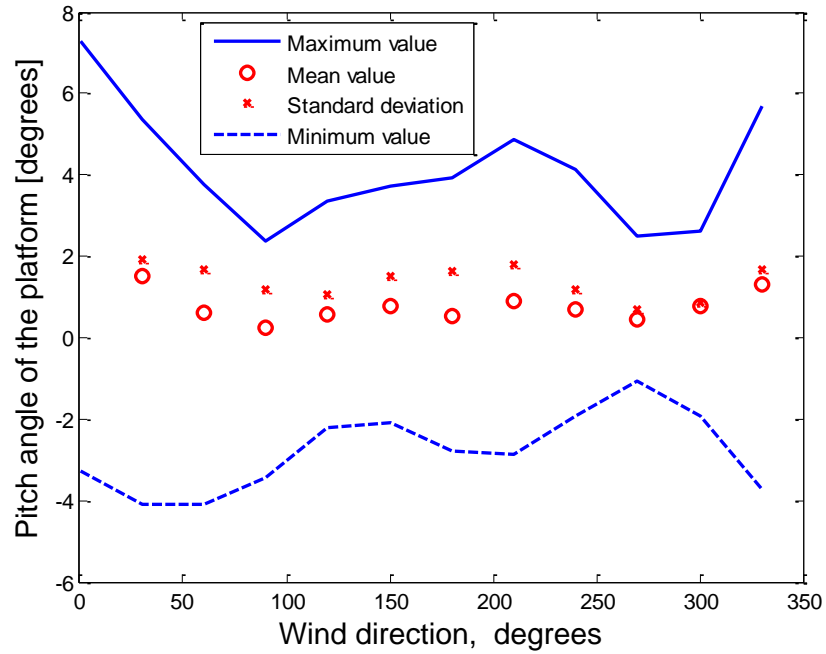
Figure I.18 – Pitch angle of the platform.

As mentioned before, the thrust force is minimal with the blades pitched to 90 degrees as can be inferred in Figure I.19, where the magnitudes are an order of magnitude lower than the steady operating thrust.
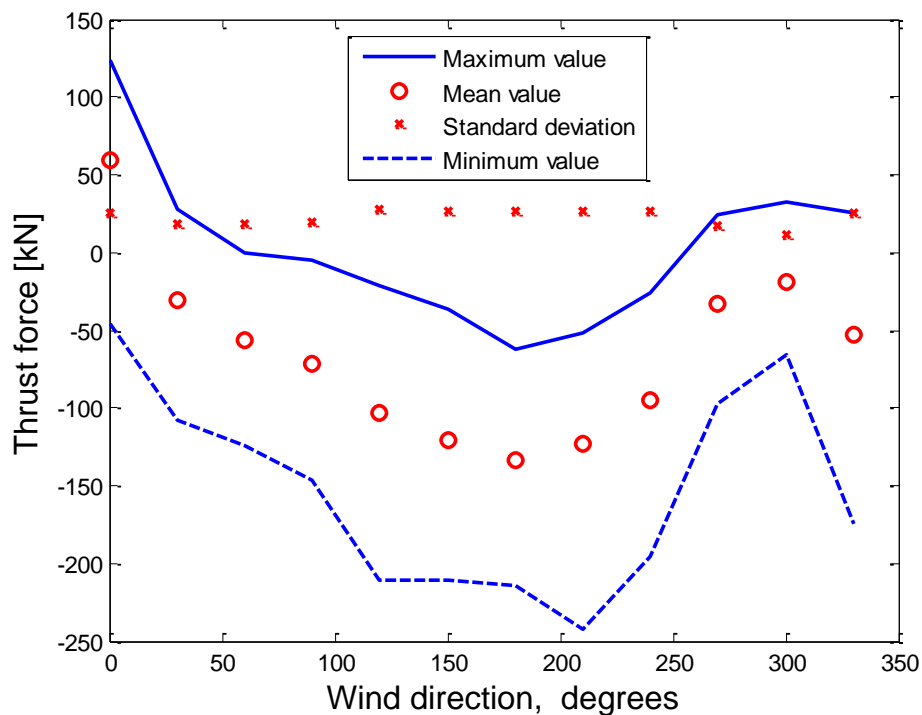

Figure I.19 – Thrust force at the rotor.

(INNWIND.EU, Deliverable 4.3.3., Innovative Concepts for Floating Structures)

Conceptual conclusions and outlook

Detailed performance assessment of an innovative 10MW floating turbine at 50 m water depth mounted on an articulated joint at the sea floor was performed. The floater comprises of 1) cylindrical spar, 2) buoyancy chamber, 3) ballast, 4) supported by 6 mooring lines and 5) the articulated joint at the sea floor.

The steady power, thrust performance curves under normal operation were satisfactory. Detailed fully coupled aero-hydro-elastic simulations shows that the loads on the support structure stay bounded for all mean wind speeds under normal turbulence and that the platform pitch motion is stable and small. Extreme storm simulations confirmed that the platform was stable even when the turbine was idling and when the control system was non-operational. Further large waves do not cause large deflections of the structure.

The results demonstrate that the 10MW semi floating turbine at 50 m water depth is functioning appropriately and can be assessed for further detailed design considerations. The TRL level for this concept is in the order of 2.

(INNWIND.EU, Deliverable 4.3.3., Innovative Concepts for Floating Structures)

PART II: CONCRETE FLOATER DESIGN (USTUTT)

Introduction

Despite the fact that steel is the most used material in marine structures concrete has also been used in the marine environment. The main reason for its low use is that concrete structures have a bigger displacement volume increasing displacement cost in case of vessels. However, O&G industry has other requirements. Recent advances in concrete technology helps to establish this material as an alternative to steel, especially in very large static structures due its low material and maintenance cost compared to steel.

The first concrete platform design, the Ekofisk Tank, see Figure II.2, was developed in 1973 for the Norwegian North Sea waters at 71 m water depth. Since then other designs have been developed as the Coondeep (concrete deep water structure). These kind of platforms rest on the sea floor thanks to a large base which is used to storage oil. From the base a variable number of columns rise even more than 100 m being the support of the platform deck. Two platforms of this type have the world record of being the tallest and largest structure ever moved, Troll B, Figure II.1, with a total height of 472 m and Gullfaks C with 836.000 t, respectibly.

Figure II.1 – Troll B semi-submersible platform, [32].

Figure II.2 – Ekofisk Tank, [32].

Concrete has the advantage for offshore wind turbine foundations that it is very resistant towards fatigue loading. Therefore the lifetime of the foundation can be crucially extended as compared to steel foundations, see [9]. The higher mass and displaced volume of water yield by far higher inertia values as compared to floating steel structures. This results in larger rigid-body eigenperiods of the floating system, needs to be taken into account especially when designing the mooring system. However, the decrease of the resonance frequency is generally desired since it brings catenary-moored systems out of the frequency range of most wave spectra.

Offshore concrete structures have shown to be very resistant and durable in the marine environment. Pre-stressed concrete of high density allows resisting the high bending loads, especially at the tower base of the wind turbine.

The differences as compared to concrete foundations for offshore wind turbines are the extended lifetime and therefore a higher initial investment cost. Although the manufacturing cost is low compared to steel the availability of a large dry dock close to the intended site is necessary.

(INNWIND.EU, Deliverable 4.3.3., Innovative Concepts for Floating Structures)

Especially for large offshore wind turbines a floating substructure of concrete with low draft and a simple shape is regarded to help driving down the foundation CAPEX.

Design concept

The proposed shape of the floating platform can be classified as a spar with modifications to allow a reduction of the overall draft. This makes the concept more flexible to the site and opens markets of shallow coastlines such as those appearing widely in Europe. A spar-type floater gains the restoring moment and stability through a center of gravity at a low position. A large metacentric height of a lightweight platform can achieve enough restoring for resisting the thrust forces of a 10MW wind turbine. Such a design would be a very slender cylinder of a draft of more than 150 m. This makes the concept little attractive for the application in sites with different water depths.

The low material cost of concrete and its requirement of simple shapes yield a spar-type platform. The USTUTT concept bases on these advantages and has the prospect of a decreased draft due to the bigger diameter compared to common spar-shapes.

In order to increase the radius of the spar while ensuring limited vertical wave excitation forces (Froude-Krylov forces) a torus-like shape is chosen, see Figure II.3.
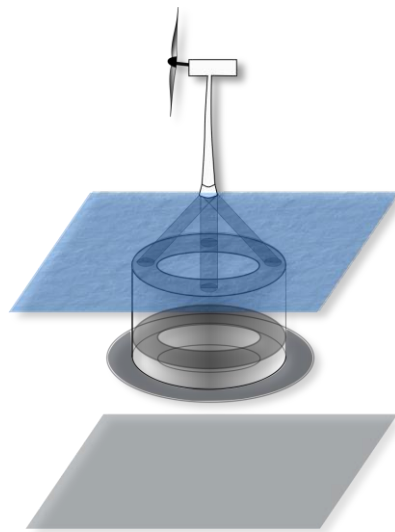

Figure II.3 – USTUTT spar: Conceptual Sketch.

The interface between the concrete torus and the tower base is assumed to be realized with three to four steel struts and bedplates for a spatial introduction of the sectional forces to the concrete body. The dimensioning of this interface, however, has not been done yet and is out of the scope of this design stage.

Design Results

The pre-design of the concrete structure involves hydrostatic and hydrodynamic analyses together with material cost estimations. They will be described in the following starting with the hydrostatic calculations.

(INNWIND.EU, Deliverable 4.3.3., Innovative Concepts for Floating Structures)

Hydrostatic analyses

The first requirement is the hydrostatic restoring as mentioned in chapter "Design Assumptions" is the hydrostatic restoring in order to ensure a limited pitching angle of the platform under a given thrust force (see above). Therefore the geometric design space of the torus-shaped spar has been calculated with the requirement of the hydrostatic restoring of $C_{55} = 2.922E9$ Nm/rad including the gravitational forces of the 10MW reference wind turbine. Applying an optimization algorithm three platform parameters have been varied while maintaining the fixed constraint of the hydrostatic stiffness C_{55}. The varied parameters are the inner radius of the torus r, the outer radius R and the platform height h equal to the draft. The calculations have been conducted based on a wall thickness of the reinforced concrete of $b = 0.5$ m which is slightly higher than the value used in [9]. The density of the reinforced concrete is assumed to be $\rho_{reinfconc} = 2750$ kg/m^3, which is a slight overestimate in order to account for additional secondary structures. The density of the ballast is $\rho_{ballast} = 2500$ kg/m^3 (black slag).

The design space for varying inner radii r and outer radii R, the resulting draft of the structure for the given hydrostatic restoring and the resulting estimated material cost can be seen in Figure II.4. It will be described and analyzed in the following.

Generally, when reducing the draft of a spar, the radius needs to increase which yields a quadratic increase of the displaced water mass. Due to the higher mass the desired hydrostatic restoring C_{55} can be achieved with a smaller metacentric height, see Equation (1). As a consequence the amount of material also increases significantly as the radius increases. This shows that the flexibility that is gained through a lower draft has to be bought with the drawback of a bigger amount of structural and ballast material.

This mechanism can be clearly seen when looking at the platform draft in Figure II.4 for a small inner radius r and increasing outer radii R. For bigger inner radii r, however, the loss of platform draft needs to be achieved through a significantly larger outer radius R as if r is small.

Looking at the material cost, again, for the small inner radius r the cost increases more or less linearly with the outer radius R whereas the material cost is approximately constant for a given R and an increasing r. The material cost as function of platform draft shows an increase for increasing inner and outer radii. A low draft requires always a high outer radius R but a small inner radius r yields always the smallest material cost for a given draft.

An optimal layout in this scenario is the one with the lowest material cost and the lowest draft. It is evident that the material cost is an easily ratable quantity. On the other side it is harder to rate the platform draft in terms of an economic benefit, since it might conditionally increase the attractivity of the concept for shallower sites but not necessarily. Nevertheless a reasonably low draft should be selected for the concept in order not to limit the possible market to only those of extremely steep coastlines as in Japan and Norway.

The sensitivity to the wave excitation has not been regarded yet, as it is a result of the potential flow calculations. However, it is likely that the vertical excitation force per unit mass of the floater will increase for a higher projected horizontal surface of the geometry. This is why also the geometries with a higher material cost that have therefore a nonzero inner radius r will be considered in the following.

For the further analyses a number of candidate structures will be selected. The hydrodynamic properties will be calculated for two scenarios. First, three platform candidates with a variable platform draft but constant material cost are selected (*VarDraft*). Second, two more platform candidates are selected with a variable material cost and a constant draft are chosen (VarCost), see Figure II.5. The data of the candidate geometries is given in Table II.1.
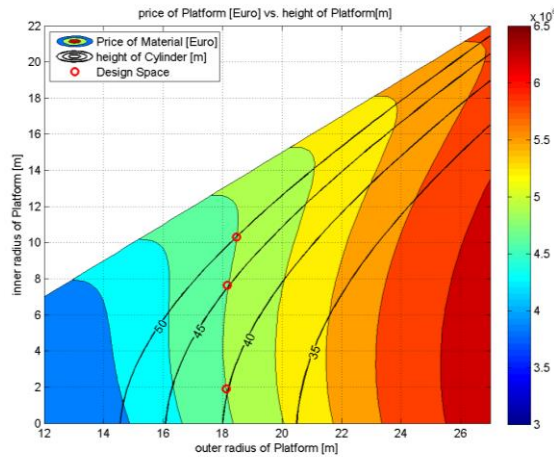

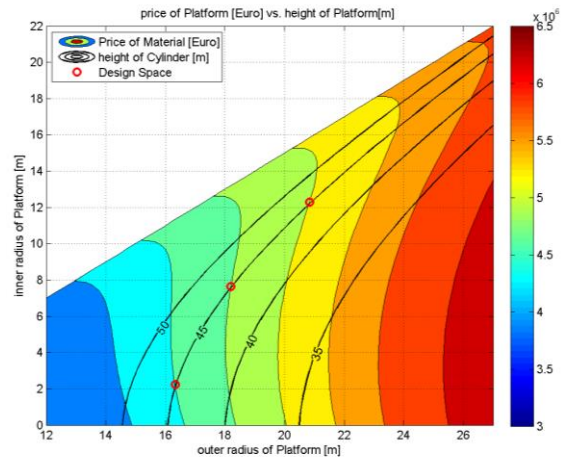Figure II.4 – USTUTT spar: Hydrostatic design space (*VarDraft*).

Figure II.5 – USTUTT spar: Hydrostatic design space (*VarCost*).

(INNWIND.EU, Deliverable 4.3.3., Innovative Concepts for Floating Structures)

Table II.1 – USTUTT spar: Properties of candidate geometries

	VarDraft			VarCost		
	H50	H45	H40	H45-1	H45-2	H45-3
Outer Radius R [m]	18.5	18.2	18.1	16.3	18.2	20.8
Inner Radius r [m]	10.4	7.7	1.7	2.2	7.6	12.3
Draft h [m]	50.0	45.0	40.1	45.0	45.0	45.0
Mat. Price [MEuro]	4.9224	4.904	4.898	4.6039	4.8998	5.2005
Restoring C_{33} [N/m]	1334201	1334201	1334201	1334201	1334201	1334201
Restoring C_{55} [Nm/rad]	2.92×10^9	2.92×10^9	2.92×10^9	2.92×10^9	2.92×10^9	2.92×10^9
Still-water eigen-period $T_{eig,33}$ [s]	47.832	49.00311	50.43153	48.0054	48.9803	49.95453
Still-water eigen-period $T_{eig,55}$ [s]	46.54995	44.40371	42.31852	43.3579	44.3978	45.74245
Total platform mass m_{ptfm} [kg]	3.74×10^7	3.937×10^7	4.17×10^7	3.8×10^7	3.93×10^7	4.095×10^7
Ballast mass $m_{ballast}$ [kg]	3.698×10^7	3.89×10^7	4.13×10^7	3.73×10^7	3.87×10^7	4.049×10^7
Platform inertia I_{55} [kgm^2]	1.02×10^{11}	9.35×10^{10}	8.55×10^{10}	9×10^{10}	9.34×10^{10}	9.8×10^{10}
Vert. dist. from platform base to platform center of gravity $z_{cm,p}$ [m]	-46.0839	-43.0199	-39.9226	-43.4684	-43.0441	-42.6889
Vert. dist. From platform base to FOWT center of gravity $z_{cm,fowt}$ [m]	-41.9124	-39.1367	-36.3436	-39.4082	-39.1566	-38.9618
Metacentric height M [m]	7.707101	7.343124	6.933043	7.65151	7.349942	7.066077

Potential Flow Calculations

Linear potential flow calculations have been performed for the candidate concepts with the software Ansys Aqwa, see [20] and comparisons made with the software Nemoh, see [33]. The shapes are initially drawn in the software Ansys Workbench and then parametrized in Ansys APDL for an automated process. The geometry in Ansys Aqwa can be seen in Figure II.6 with the mesh visualized in Figure II.7. All rotational quantities calculated are given with the overall center of gravity as a reference.

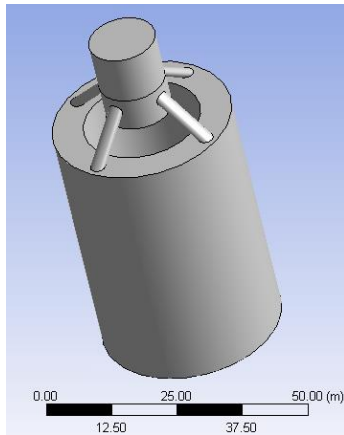*(INNWIND.EU, Deliverable 4.3.3., Innovative Concepts for Floating Structures)*

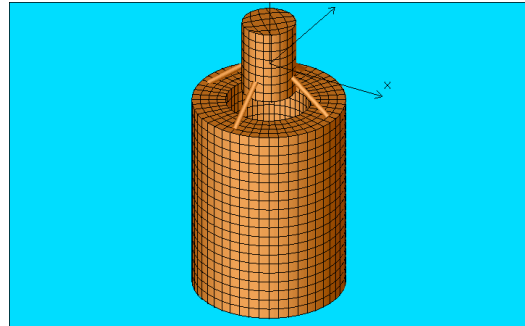Figure II.6 – USTUTT spar: Example geometry as Ansys model.

Figure II.7 – USTUTT spar: Mesh in Ansys Aqwa.

Figure II.8 and Figure II.9 show the response amplitude operators (RAO) in heave and pitch direction, respectively. The RAOs are shown for drafts from $h = 35 \ldots 50$ m together with a common wave spectrum as a reference. It can be seen that there exists a sharp peak at low frequencies of around 0.15 rad/s. In the frequency range of the wave spectrum there response is rather small and comparable between the different platforms. The large amplitudes of the response around the resonance frequency will be by far smaller due to the introduced damping by the structure itself and the heave plates at the bottom of the torus, see Figure II.3.
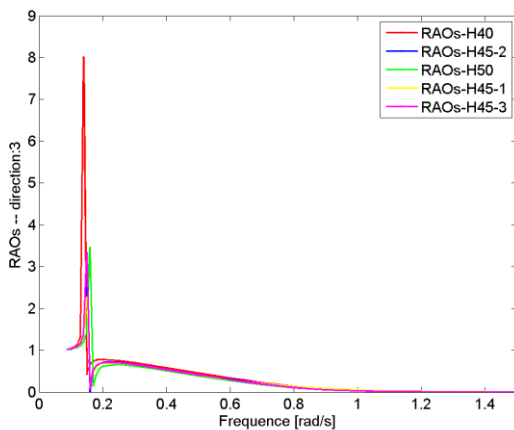

Figure II.8 – USTUTT spar: Translational RAO in vertical direction.
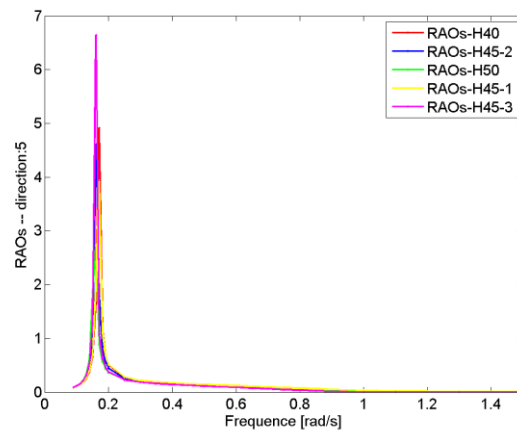

Figure II.9 – USTUTT spar: Rotational RAO in pitch direction.

The wave excitation force including diffraction forces as well as Froude-Krylov forces has been calculated and normalized with the total displaced water mass for each concept. The wave excitation force or *Force RAO* is the total force exerted on the structure by regular wave of norm amplitude. It does not depend on the mass properties and is therefore a measure of the sensitivity of the hull shape to wave excitation.

Figure II.10 shows the magnitude of the frequency-dependent moment in pitch-direction for the three candidates with differing draft (*VarDraft*). Figure II.11 shows the same quantity for the candidates with differing cost (*VarCost*). The plots also contain the still-water eigenfrequency for these concepts. They are introduced to the wave excitation forces in order to assess the frequency difference between the peak response frequency to wave forces and the natural frequency in water without waves. This difference should be as large as possible in order to ensure a limited response for the freely floating body in waves in the RAO.

In the case of varying draft the normalized wave excitation response is higher for the geometries with lower draft around the peak frequencies. Thus, the longer platforms receive a smaller exciting force per unit inertia. This means there is an advantage for the platforms of bigger draft. For the geometries with constant draft in Figure II.11 the excitation is higher for the shapes with smaller inner and outer radius. These are also the geometries with a higher material cost and overall inertia. The same tendency can be seen when looking at the wave excitation response without normalization. This result backs the selection of a torus shape instead of the solid cylinder because here the shapes with a bigger inner radius show the smaller wave excitation response.
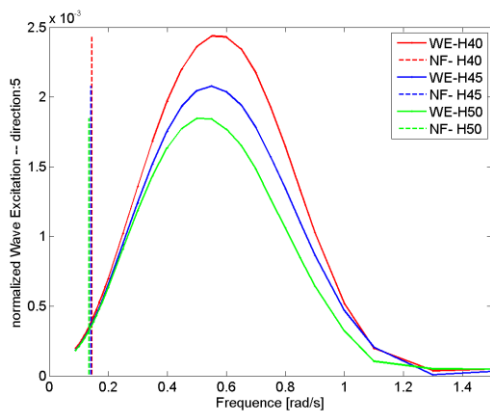

Figure II.10 – USTUTT spar: Rotational normalized wave excitation response in pitch (*VarDraft*).
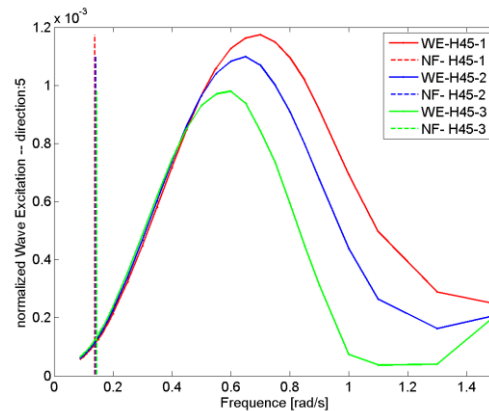

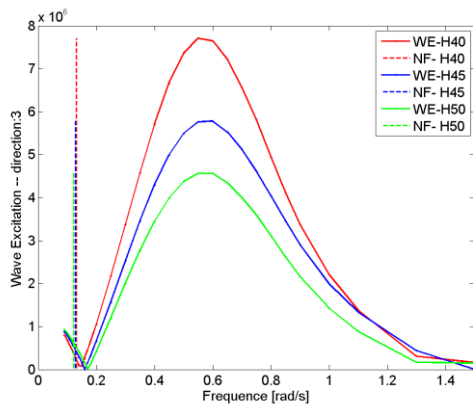Figure II.11 – USTUTT spar: Rotational normalized wave excitation response in pitch (*VarCost*).

Figure II.12 – USTUTT spar: Translational normalized wave excitation response in heave (*VarDraft*).
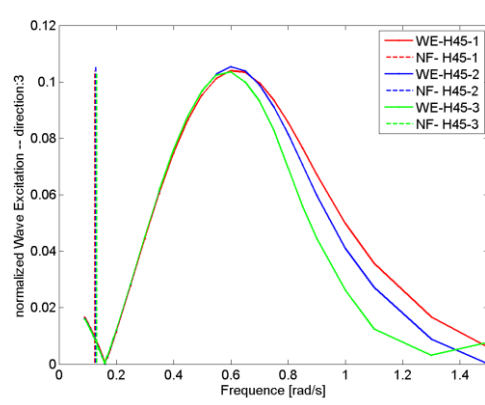

Figure II.13 – USTUTT spar: Translational normalized wave excitation response in heave (*VarCost*).

(INNWIND.EU, Deliverable 4.3.3., Innovative Concepts for Floating Structures)

Figure II.12 and Figure II.13 show the wave excitation force in vertical direction. Here the candidate with the largest draft shows the highest excitation. The reason is here most probably the large projected horizontal surface of this shape. The concepts with constant draft and varying cost in Figure II.13 feature a comparable wave excitation response.

From this analysis it can be said that the candidate structures show a fairly comparable RAO and also the sensitivity to wave excitation is comparable. A structure with the advantage of a low draft might even be favourable in terms of the wave excitation response. When the draft is held constant and the radii are varied (or the material cost) the effects are hard to judge, which is most likely due to the coupled change of the projected horizontal hull surface and the structural inertia.

From this analysis the shapes with a bigger draft and a relatively large inner radius are favourable. Further specifications on the site will determine the relevant draft of the system for further calculations and concept development.

Conceptual conclusions and outlook

A torus-shape concrete spar platform with different dimensions, all suitable for supporting the InnWind.EU 10MW reference wind turbine has been evaluated in terms of a pre-design. The potential flow calculations show that the response to wave excitation is for all assessed geometries very low in the range of a typical wave spectrum. All shapes feature a sharp peak for very low frequencies. It is therefore planned to decrease the magnitude of this peak through damping plates at the bottom of the structure. Nevertheless, the mooring system will have to be designed thoroughly in order to avoid a low-frequency excitation of the system due to slow drift forces.

The material cost of about 0.5 M€/MW is considered reasonable and allows further development of the concept. The manufacturing and installation conditions will have to be determined in order to further assess the required maximum draft and the additional costs for dry-dock manufacturing and transportation.

The next steps will include coupled hydro-aero-servo-elastic simulations including an iterative adaptation of the mooring system and the damping plates. For these simulations the blade-pitch controller will have to be adjusted for the platform shapes. Also the environmental conditions will have to be determined in order to eventually evaluate the coupled system and compare the dynamic behaviour.

With the presented calculations the uncoupled hydrostatic and hydrodynamic suitability of the concept has been shown. The dimensions (draft, diameter) and material cost is reasonable. Also the fabrication of such a design in pre-stressed concrete is regarded as feasible. This stage can be classified as TRL 1.

PART III: SEMI-SUB FLOATER DESIGN #1 (CENER)

Introduction

In this chapter, a floating platform concept developed by CENER for the INNWIND 10MW wind turbine [13] is presented. The design conditions for the platform are described in detail in [34]. A fixed pitch hydrostatic stiffness of 2.992E9 Nm/rad is defined in that document. This stiffness will result in a pitch displacement of the platform of 3.5 deg under the steady rated wind speed. A slight modification is introduced in the INNWIND 10MW wind turbine model: the tower has to be cut at a height of 12 m due to the freeboard of the platform. The resulting total mass of this modified wind turbine is **$1.144 \cdot 10^6$ kg** .The depth of the sea location is 200 m.

A semisubmersible platform design has been selected for the several reasons:

- Well proven concept in the Oil & Gas industry
- Less installation cost
- Easy assembly turbine-platform both onshore and offshore
- Easy in site installation
-

Design concept

The platform basically consists on an equilateral triangle with three stabilizing columns, one in each vertex joined by three pontoons. The wind turbine is located in one of the columns, to avoid the use of an additional central column.

The platform design presented reduces the number of elements in the water plane, minimizing the hull cross section area at the sea surface where wave energy is located. The material and construction cost is reduced avoiding bracings and other connecting structural elements. The center of gravity is lowered to increase stability through the use of sea water as ballast.

Figure III.1 presents a tridimensional model of the concept design:

Figure III.1 – Isometric view of the proposed platform

(INNWIND.EU, Deliverable 4.3.3., Innovative Concepts for Floating Structures)

The main geometric characteristics of the platform are presented in Table III.1 :

Table III.1 – Platform main characteristics

Main characteristics	
Distance between columns	66 m
Draft	25.5 m
Platform depth	37.5 m
Freeboard	12 m
Column diameter	14.5 m
Pontoon breadth	10.875 m
Pontoon depth	7 m
Buoyancy volume	24907 m^3
Center of buoyancy	0, 0, -17.32 m

Figure III.2 illustrates the main dimensions of the platform. The origin of the reference system is located in the geometric centre of platform and at the sea water level (SWL). All the physical properties and results will be referred to this reference system.
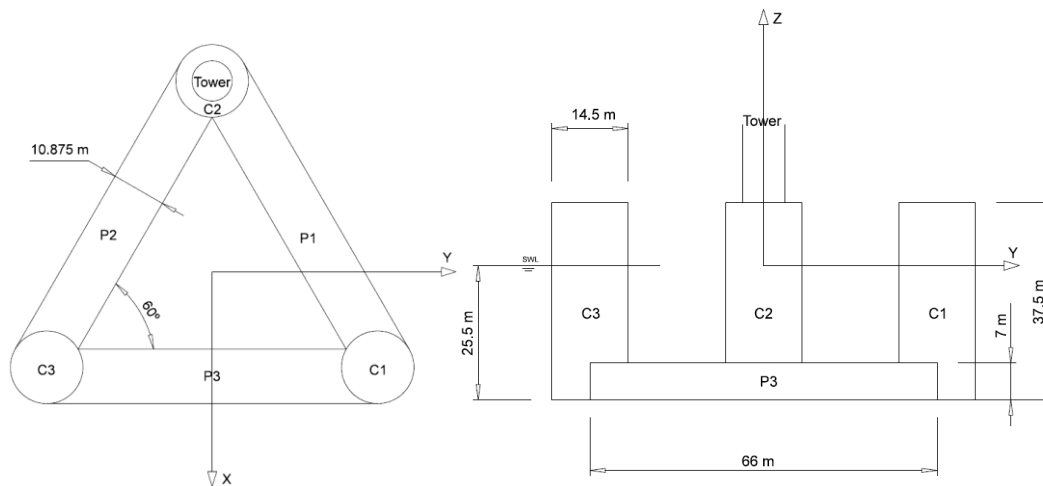

Figure III.2 – Plan (left) and Side (right) view of the platform

Design Results

Methodology

In this section it is explained the assumptions, methodology and software used for the different calculations and for the design of the concept.

Mass estimation

A constant thickness of 6cm in all the platform walls has been considered to estimate the total steel weight to get the appropriate position of the centre of gravity during the design of the platform, it has been ballasted with sea water with a density of 1025 kg/m³.

Hydrostatic

The hydrostatic heave stiffness (C_{33}) and pitch stiffness (C_{55}) can be calculated by the following expressions [35]:

$$C_{33} = \rho g A_{wp} \tag{1}$$

$$C_{55} = \rho g V (Z_B - Z_G) + \rho g \iint x^2 ds \tag{2}$$

Where:

- ρ: Sea water density
- g: Gravitational acceleration
- A_{wp}: Waterplane area of the platform
- V: Buoyancy volume
- Z_B: Center of buoyancy height from SWL
- Z_G: Center of gravity height from SWL
- $\iint x^2$ ds: Second moment of area of the horizontal cross section at SWL

According to Equation (2), the pitch stiffness has contributions from the gravity, the buoyancy and the waterplane area. These components will be presented separately on the results in Section "Hydrostatic pitch and heave stiffness".

Stability

Sesam_HydroD has been used to calculate the stability performance. Assuming a small pitch angle the heeling arm can be analyses with Equation (3):

$$GZ = GM_L \, Sen \, \theta \tag{3}$$

The righting moment M_R has been calculated with Equation (4):

$$M_R = GZ \, \rho g v \tag{4}$$

Still-water eigenperiod

The heave and pitch eigenperiods of the platform have been calculated using the following expression:

(INNWIND.EU, Deliverable 4.3.3., Innovative Concepts for Floating Structures)

$$T_{ni} = 2\pi \sqrt{\frac{M_{ii}+A_{ii}}{C_{ii}}} \qquad (5)$$

For the heave eigenperiod ($T_{eig,33}$) the different parameters are:

- M_{33}: Total platform mass
- A_{33}: Added platform mass for heave degree of freedom
- C_{33}: Heave hydrostatic stiffness

And for pitch eigenperiod ($T_{eig,55}$) the parameters are:

- M_{55}: Platform inertia around Y axis
- A_{55}: Added platform inertia around Y axis
- C_{55}: Pitch hydrostatic stiffness

For the calculation of the natural periods, the platform added mass has been taken from the analysis that is explained in the next Section "Seakeeping and manoeuvring".

Seakeeping and manoeuvring

WAMIT potential code [21] has been used to calculate the added mass and damping coefficients (manoeuvring) and the force coefficients (seakeeping). The same software has been used to compute the motion RAO's.

Mooring system

The mooring system has not being designed. Instead, we have performed the calculations using the 6x6 stiffness matrix of the OC4 mooring system [36].

We have also considered the contribution of this mooring system to the total mass though, in comparison with the total platform and wind turbine weight, it is rather small: $1.875 \cdot 10^5$ kg.

Cost estimation

The platform material cost has been calculated considering a steel thickness of 6 cm in all platform walls. There is no fixed ballast material in the design.

The estimated cost per ton of steel including construction is 300 0€ [34].

Concept performance and results

The methodology described in the previous Section "Methodology", has been applied to calculate the results presented in this section: system mass, hydrostatic stiffness, still-water eigenperiods, motion RAO's, wave excitation forces and material cost.

System mass

The total system mass is presented in Table III.2. The assumptions for this mass estimation have been explained in Section "Mass estimation". Together with the total mass, the wind turbine (tower, nacelle, hub and blades), platform, ballast and mooring system masses are presented separately:

(INNWIND.EU, Deliverable 4.3.3., Innovative Concepts for Floating Structures)

Table III.2 – System masses

System mass	
Wind turbine	$1.144 \cdot 10^6$ Kg
Unballasted platform	$5.714 \cdot 10^6$ Kg
Ballast	$1.849 \cdot 10^7$ Kg
Mooring system	$1.875 \cdot 10^5$ Kg
Total mass (m_{FOWT})	$2.553 \cdot 10^7$ Kg

The platform ballast is exclusively composed by sea water. The ballast distribution is shown in Table III.3:

Table III.3 – Ballast distribution

Ballasting			
Tank	Total volume	Filling fraction	Fluid volume
Column 1 (C1)	6187.6 m³	44.3%	2741.12 m³
Column 2 (C2)	6187.6 m³	26.2%	1621.19 m³
Column 3 (C3)	6187.6 m³	44.3%	2741.12 m³
Pontoon 1 (P1)	4094.9 m³	89%	3644.48 m³
Pontoon 2 (P2)	4094.9 m³	89%	3644.48 m³
Pontoon 3 (P3)	4094.9 m³	89%	3644.48 m³

The system inertias are presented in Table III.4 in the reference system defined in Figure III.2:

Table III.4 – System inertias

System inertias	
Ixx	$3.105 \cdot 10^{10}$ kgm²
Iyy	$3.103 \cdot 10^{10}$ kgm²
Izz	$2.373 \cdot 10^{10}$ kgm²

Hydrostatic pitch and heave stiffness

Table III.5 shows the total hydrostatic pitch stiffness and also the contributions from buoyancy, gravity and the waterplane area calculated with Equation (2):

(INNWIND.EU, Deliverable 4.3.3., Innovative Concepts for Floating Structures)

Table III.5 – Pitch hydrostatic stiffness

Pitch hydrostatic stiffness	
Contribution from buoyancy	-4.334·10^9 Nm/rad
Contribution from gravity	3.585·10^9 Nm/rad
Contribution from waterplane area	3.674·10^9 Nm/rad
C_{55}	2.925·10^9 Nm/rad

In addition, Equation (1) has been used to calculate a heave stiffness of 4.967·10^6 N/m.

Stability

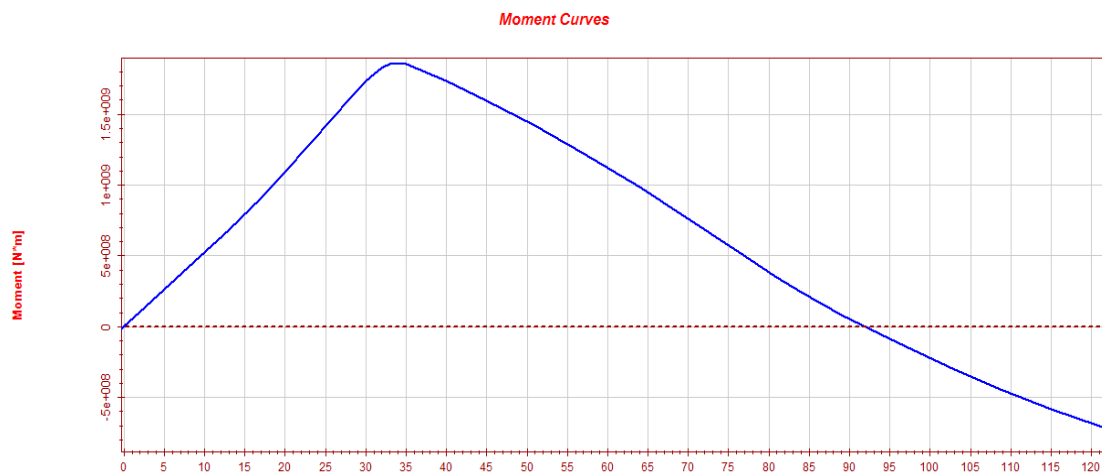Figure III.3 shows the righting moment curve against the inclination angle of the platform:

Figure III.3 – Platform righting moment

The righting moment increases with the inclination angle until it reaches a maximum close to 2.0·10^8 Nm around 34deg. For higher values of inclination, the righting moment decreases until 92 deg, where the platform would capsize. For an inclination angle of 3.5 deg the righting moment equals the maximum heeling moment (1.785·10^8 Nm) produced by the rotor thrust at the rated wind speed, which is consistent with the design conditions defined in [34].

Still-water eigenperiods

The heave and pitch eigenperiods have been computed with equation (5) and the results are presented in Table III.6:

Table III.6 – Still-water eigenperiod

Still-water eigenperiod	
$T_{eig,33}$	20.66 s
$T_{eig,55}$	24.41 s

The resulting natural periods are higher than 20 s to avoid the periods with more energy of typical wave spectra. If it were necessary, the periods could be increased with a slight redesign of the platform.

Heave and Pitch RAO's

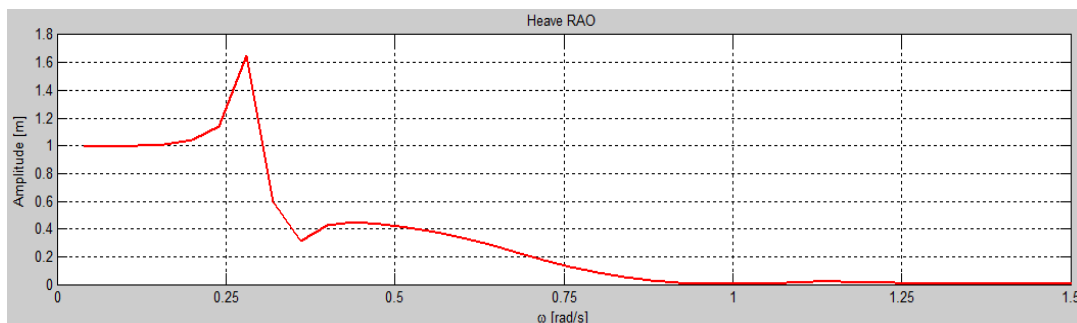Figure III.4 shows the heave RAO in the nominal wave direction.

Figure III.4 – Heave RAO for nominal direction

The plot shows that for very low values of angular frequencies (until 0.13 rad/s) the heave response is 1 meter, because the wave length is higher than the platform dimensions. The maximum response appears at a wave frequency close to the heave natural frequency. Finally, for high wave frequencies (higher than 1 rad/s) the platform response in heave is low.

Figure III.5 represents the platform pitch motion RAO in the wave nominal direction.
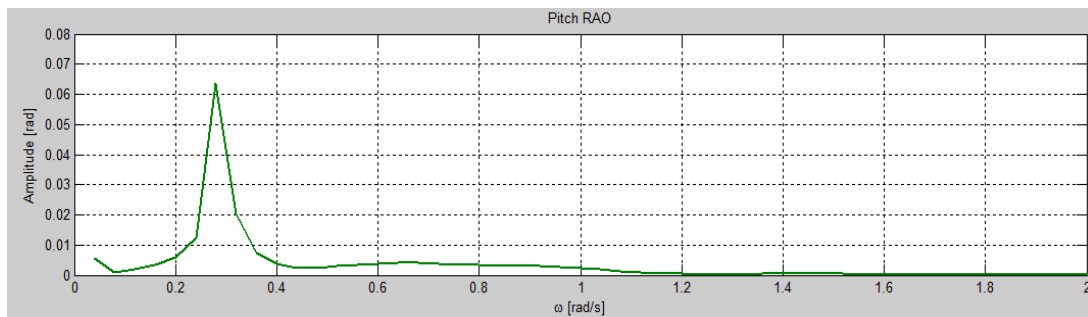

Figure III.5 – Pitch RAO for nominal direction

The maximum pitch response appears at a wave frequency of approximately 0.28 rad/s, which is close to the pitch natural frequency.

(INNWIND.EU, Deliverable 4.3.3., Innovative Concepts for Floating Structures)

Wave excitation force

Figure III.6 shows the excitation force in the surge degree of freedom divided by the total floating offshore wind turbine mass, m_{FOWT}, **that was presented in** Table **III.4:**
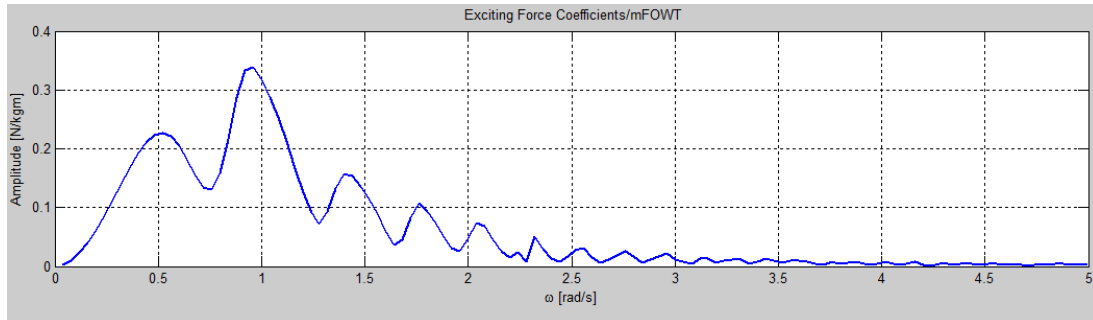

Figure III.6 – Surge excitation force divided by total floating offshore wind turbine mass

The maximum surge excitation force is located at wave frequency of approximately 0.9 rad/s (7 s of wave period).

Similarly, Figure III.7 shows the excitation moment in the platform pitch degree of freedom divided by the total inertia in pitch that was presented in Table III.4.
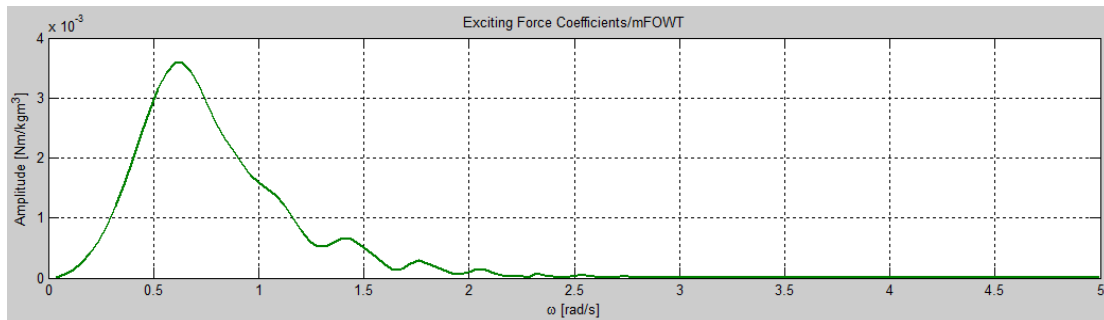

Figure III.7 – Pitch excitation force divided by floating offshore wind turbine inertia

Material cost

Table III.7 summarizes the cost estimation of the platform design. The weight of the platform was presented in Table III.2 and the assumptions of this calculation were explained in Section "Mass estimation".

Table III.7 – Material cost

Material cost	
Material	Steel
Material cost per ton	3000 €/t
Platform steel weight	5709 t
Total cost	17,127,000 €

(INNWIND.EU, Deliverable 4.3.3., Innovative Concepts for Floating Structures)

Conceptual conclusions and outlook

A new conceptual design of a floating platform for a 10MW wind turbine has been proposed. A preliminary evaluation of the concept has been presented. The design presents natural frequencies out of the higher energy frequencies of a typical wave spectrum. The motion and force RAO's show a good performance of the platform with moderate excitation in all the range of wave frequencies considered.

The total mass of the platform is $2.553 \cdot 10^7$ Kg, including the water ballast and the wind turbine. The mass of steel is for the platform is 5709 t. Based on this mass, we have estimated an approximate manufacturing cost of the platform of 17 M€. Though it is a very rough estimation, it is a reasonable value for a 10MW steel platform.

The simulations and results presented in this document are preliminary. Though the performance of the design proposed seems very promising, further testing and analysis is required. Therefore, we estimate a Technology Readiness Level (TRL) of 2.

(INNWIND.EU, Deliverable 4.3.3., Innovative Concepts for Floating Structures)

PART IV: SEMI-SUB FLOATER DESIGN #2 (NTUA)

Introduction

The conceptual design investigation carried out at NTUA aimed at considering different variants that ensure suitability in a wide range of depths. Semi-submersible floaters use buoyancy in order to produce the necessary restoring moment and this allows achieving smaller drafts as compared to spar-buoys in which restoring is generated by means of ballast. Therefore, targeting a wide range of depths, concepts of the semi-submersible type are more suitable. The border line between the two is not restricting and mixed systems combining ballast and buoyancy generated restoration can be considered.

In semi-submersible floaters, buoyancy is delivered by either a transparent to waves multi-cylinder system as in the WindFloat and the OC4 designs or by a closed torus-like system of cylindrical or rectangular plan form as in the IDEOL proposal. In the latter case the water within the torus can act as a damper in the heave motion. With respect to heaving a usual way to improve the response is by adding heave plates, as done in the OC4 design.

Besides the shape of the floater, of importance is the placement of the wind turbine. In the OC4 design, the wind turbine (WT) is centered while in the WindFloat and IDEAL designs, the turbine is off set. Off-setting the WT requires a balancing system based on ballast management as in the WindFloat concept which is avoided in the case of center mounting. Of course in the latter case the structural design that should withhold the WT weight and its dynamics complicates the construction.

Design concept selection

The basic element in the conducted investigation is a cylindrical torus with or without heave plates (Figure IV.1) which was considered either in combination with a spar buoy (Figure IV.2) or as the only buoyancy delivering element (Figure IV.3). The upper grey part is assumed to be made of concrete while the lower blue part is assumed to contain the ballast of the floater.
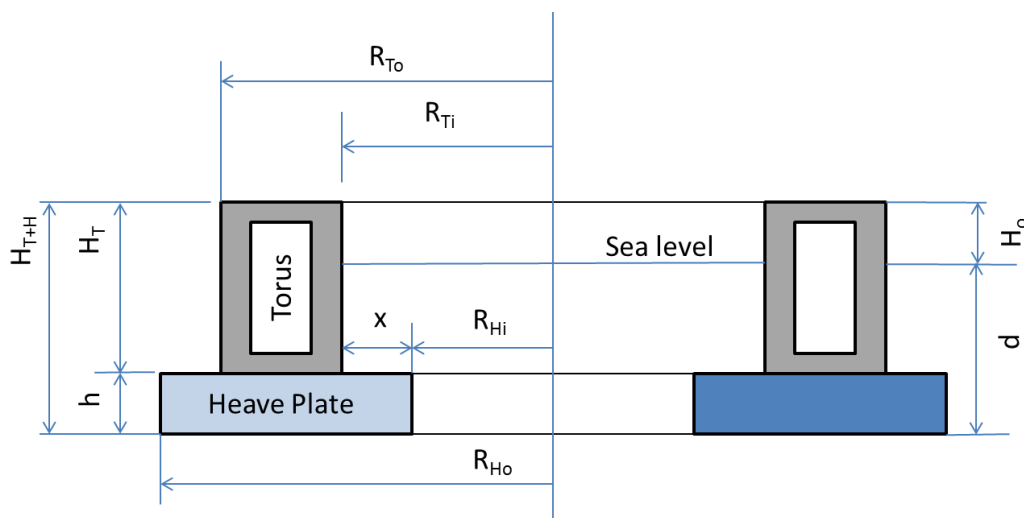

Figure IV.1 – Definition of the torus geometry

(INNWIND.EU, Deliverable 4.3.3., Innovative Concepts for Floating Structures)
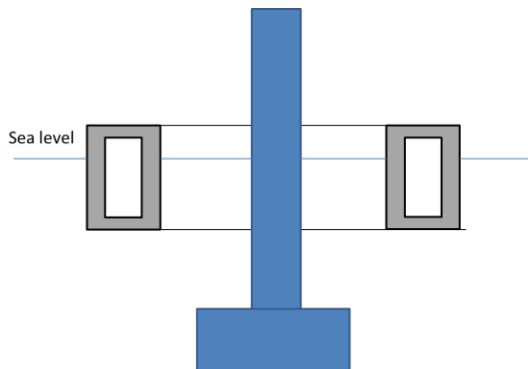
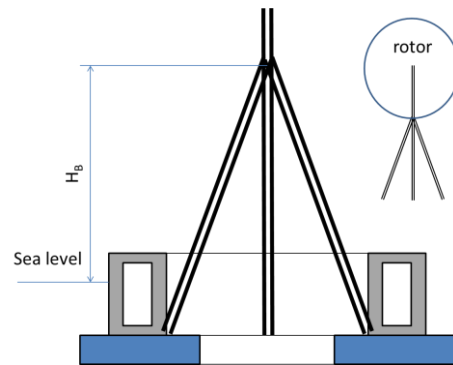Figure IV.2 – A mixed buoyancy-ballast floater (Concept 1)

Figure IV.3 – A semi-submersible torus shaped floater (Concept 2)

Concept 1 was first considered in an attempt to minimize the wave induced pitching of the WT. To this end the torus delivers part of the buoyancy and is connected to the spar-buoy with a gimbal connection so that it does not transfer moments. This means that the spar-buoy should be hydrostatically stable by itself and therefore its draft cannot be small. In the parametric study conducted it was deduced that for spar diameters in the order of that at the bottom of the tower, the reduction in draft as compared to the single spar–buoy depended on the amount of buoyancy contributed by the torus and did not exceed 25 %. Furthermore depending on the positioning of the gimbal connection, the pitching of the WT because of the horizontal force acting on the torus was not eliminated even when the connecting was set at the metacentre of the spar. So Concept 1 was not retained.

Next keeping the torus in the design, Concept 2 was considered as a one piece semi-submersible floater. As compared to multi-cylindrical floater, Concept 2 allows achieving smaller overall floater diameter and therefore offers more options regarding its construction and the way the WT is mounted on it. In Figure IV.3 the WT is mounted on the heave plate with a tripod but other options such as mounting on top of the torus or having a jacket tower instead of a tripod are possible. The choice in this respect depends on the structural requirements of the connecting brackets as function of their vertical slope which in turn is determined by the clearance of the rotor with respect to the sea level H_B. Assuming that the distance between the rotor disk and the tower is set to its minimum required value, the supporting elements between the tower and the floater should not exceed H_B.

Design Results

The work has been carried out with respect to the NREL 5MW wind turbine for which previous detailed investigations (mainly within the IEA OC* Annexes) offer a complete data base of data. It is noted that for the present conceptual design phase, the choice of the WT is not critical. The conducted analysis is linear and therefore the results and conclusions are extendable to larger WT sizes.

The analysis presented next is based on hydrostatic calculations for the dimensioning of the floater followed by linear hydrodynamic analysis. The static pitch angle was limited to 3.5 deg which was calculated for the maximum thrust of the NREL 5MW WT. For the hydrodynamic analysis, the hydrodynamic module in hydroGAST was used [37]. The

(INNWIND.EU, Deliverable 4.3.3., Innovative Concepts for Floating Structures)

specific module solves the hydrodynamic problem in integral form based on a panel surface description of the solid boundaries carrying constant source distributions and has been validated within OC4 against the WAMIT calculations.

In addition to the floater input, the gravitational, inertial and aerodynamic loads contributed by the WT are included. For the first two, the wind turbine components are modelled as concentrated masses placed at their corresponding mass centers while the aerodynamic loads are linearized with respect to the reference state corresponding to rated conditions. Let $\mathbf{q}$ denotes the vector of the 6 floater motions. Then the velocity perturbations $\delta U_a, \delta U_c$ induced by the floater motions are added in the definition of the angle of attack (Figure IV.4),

$$\tan\varphi = \frac{U_w(1-a)+\delta U_a}{\Omega r(1+a')+\delta U_c}, \quad a = \varphi - \theta_t + \beta_p$$

where U_w is the wind velocity, Ω the rotational speed, θ_t the blade twist and β_p the blade pitch. By assuming that the WT has no flexibility and that the aerodynamic induction factors a, a' remain constant, the floater motions will induce a perturbation in angle of attack $\delta\alpha$, which will give perturbations in lift and drag:

$$\delta\alpha = \partial_q\alpha.\delta q + \partial_{\dot{q}}\alpha \cdot \delta\dot{q} \quad \Rightarrow \quad \delta C_L = \partial_\alpha C_L \delta\alpha$$

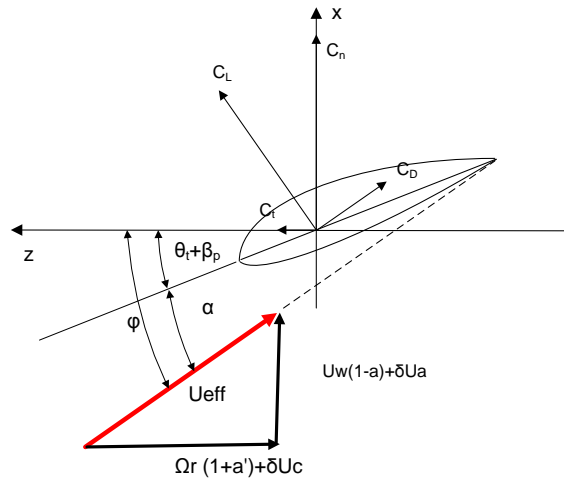where $\partial_\alpha C_{L,D}$ are calculated at the reference conditions.

Figure IV.4 – Definition of the aerodynamic set-up

Following the formalism of Lagrangian equations,

$$\frac{d}{dt}\left(\frac{\partial L}{\partial \dot{q}_i}\right) - \left(\frac{\partial L}{\partial q_i}\right) = Q_i = \sum_j \frac{\partial(\mathbf{f}_j \cdot \mathbf{r}_j)}{\partial q_i} \quad L = L(\mathbf{q}, \dot{\mathbf{q}})$$

where L denotes the Lagrangian and $\mathbf{Q}$ the generalized external loads (aerodynamic, gravitational), the mass, damping and stiffness matrices induced by the WT are obtained. Finally it is noted that in the simulations a catenary mooring has been assumed similar to that of OC4.

(INNWIND.EU, Deliverable 4.3.3., Innovative Concepts for Floating Structures)

Table IV.1 gives the basic characteristics of the designs considered next. In all cases H_o=10 m. ID=1,2,3 correspond to a simple torus (without heave plate) and differ in draft, d=10,20,30 m. The effect of the heave plate is considered with respect to ID 2,2b.2c while ID=4,5 correspond to a torus of smaller size. Cost estimations are also provided assuming construction with reinforced concrete and use of ballast (see notes at the end of the table).

Table IV.1 – Dimensions, masses and costs

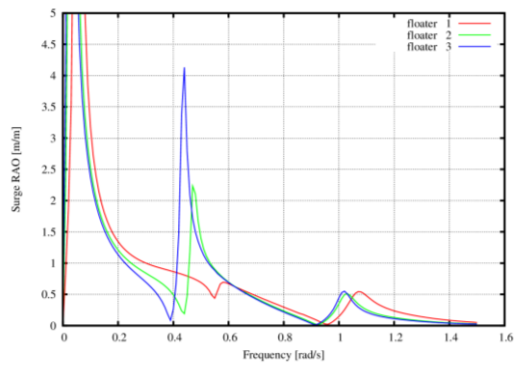| Type	ID	R_{Ti} (m)	R_{To} (m)	d (m)	h (m)	R_{Ho} (m)	x (m)	Concrete (tn) *	Ballast (tn) **	Cost (M€) ***
Torus	1	22	29	10	5	29	0	10382	326	1.6
	2	22	29	20	5	29	0	13587	8618	2.1
	3	22	29	30	5	29	0	16791	16909	2.7
	4	8	20	20	5	20	0	14816	10335	2.3
	5	8	22	10	5	22	0	16158	12229	2.5
Torus + Heave Plate	2b	22	29	20	5	35	6	9219	11633	1.5
	2c	22	29	20	5	32	3	8746	3991	1.3

* The thickness of the reinforced concrete is 0.4 m and the material density is 2500 kg/m³

** The ballast material is assumed to be mixed stones and water with density=2000 kg/m³,
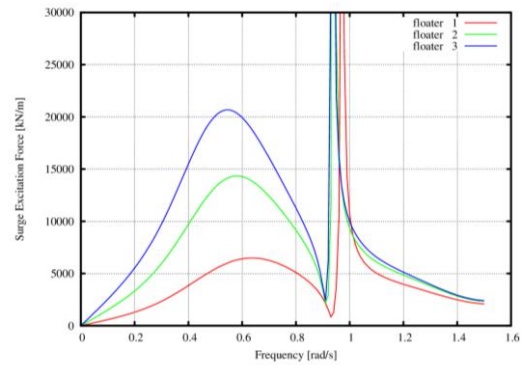
*** Concrete Cost =150 €/tn (material cost and manufacturing cost). Ballast cost: 8 €/tn. These values correspond to the real cost without any profit and were communicated by a construction company. So the actual cost is expected higher.

In the following figures, the main excitations are presented in terms of the corresponding RAOs and excitation loads, namely those in surge (Figure IV.5), pitch (Figure IV.6) and heave (Figure IV.7).
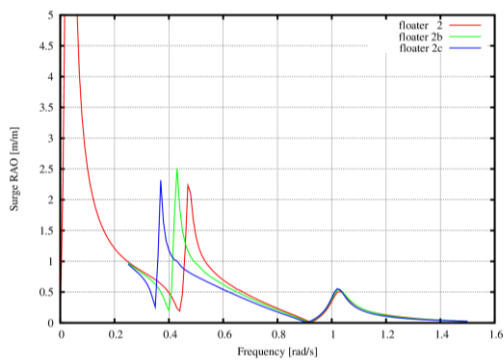
The main feature of a torus is the occurrence peak frequencies due to the waves generated within its inner area. In the surge and pitch excitation load plots (Figure IV.5, Figure IV.6), resonance occurs at ±0.95 rad/sec. Surge and pitch are closely connected which explains the similarity of the plots. For the same cross section (ID1, 2, 3), by increasing the draft, the resonating frequency moves to lower values alongside with an increase in the maximum value appearing at ±0.6 rad/sec (Figure IV.5d, Figure IV.6d). For ID2, adding heave plates to ID2 (Figure IV.5e, Figure IV.6e), increases the maximum value in the ±0.6 rad/sec increases without eliminating resonance. Then by changing the inner diameter, which comes alongside with the decrease of the outer diameter, the resonance does not appear in the frequency range considered (Figure IV.5f, Figure IV.6f). Also the loads in the ±0.6 rad/sec range remain reasonable.

(INNWIND.EU, Deliverable 4.3.3., Innovative Concepts for Floating Structures)
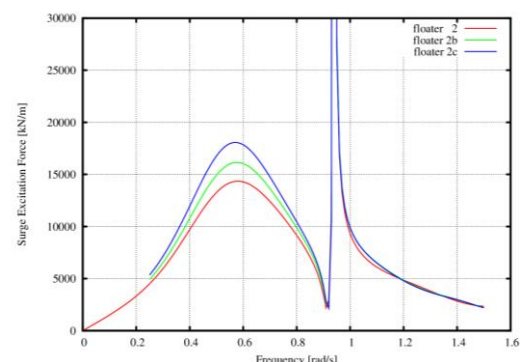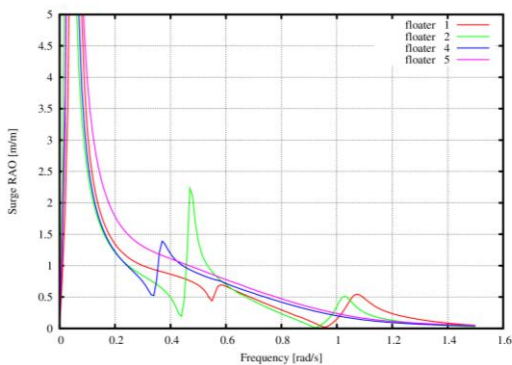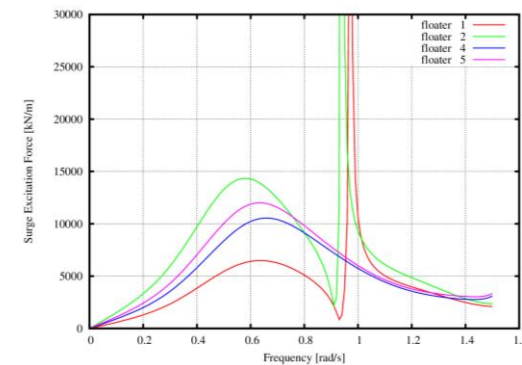
(a)

(d)

(b)

(e)

(c)

(f)

Figure IV.5 – RAOs (Left column) & Excitation Force plots (right column) in surge. Figures (a,d) show dependency on the draft for floaters with the same inner and outer diameters, Figures (b,e) show the effect of adding heave plates on the ID2 floater, and Figures (c,f) compare floaters of different dimensioning without heave plates for drafts of 10m (ID1 and 5) and 20m (ID 2,4).

(INNWIND.EU, Deliverable 4.3.3., Innovative Concepts for Floating Structures)
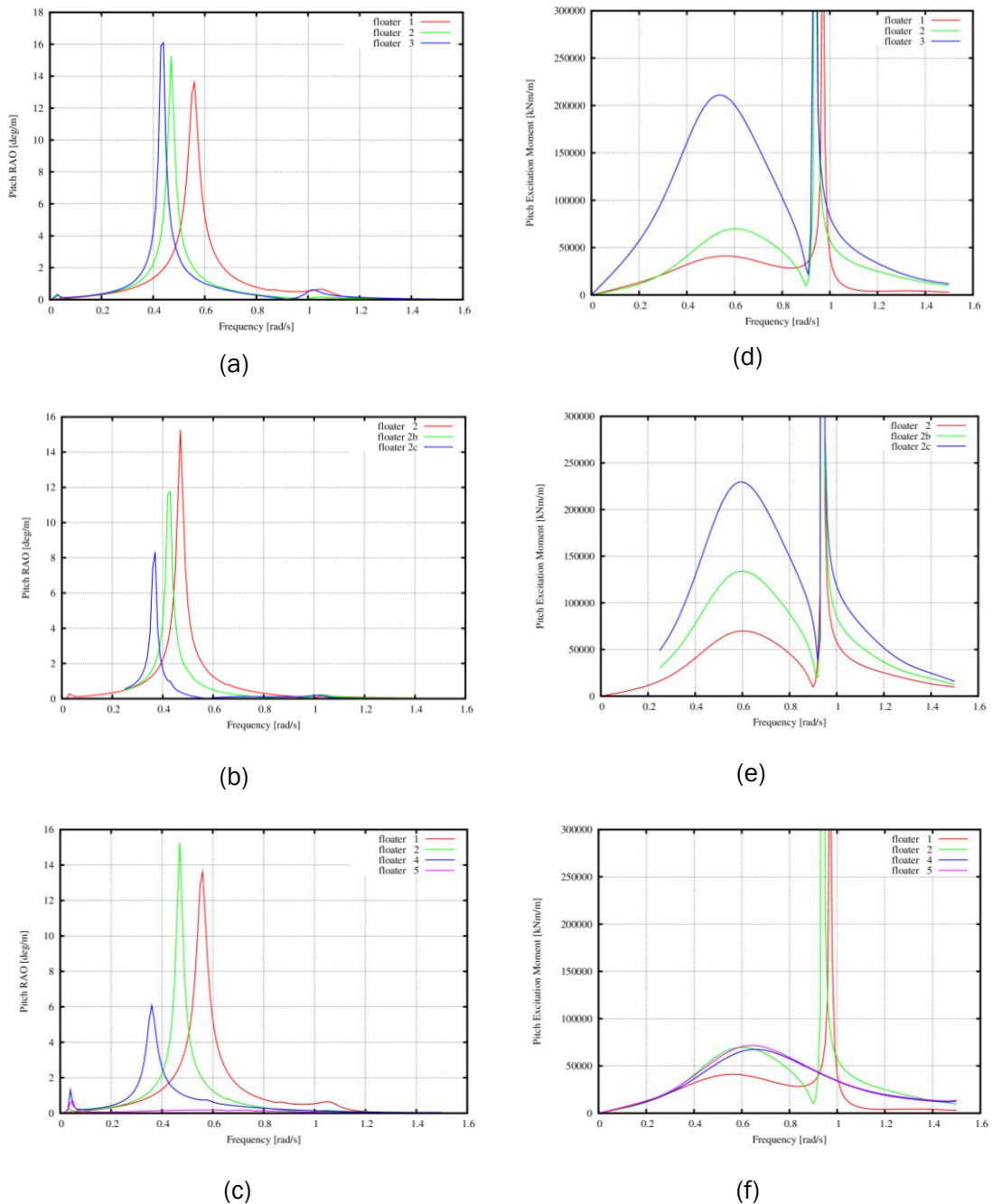
(a)

(d)

(b)

(e)

(c)

(f)

Figure IV.6 – RAOs (Left column) & Excitation Moment plots (right column) in pitch. Figures (a,d) show dependence on the draft (ID1=10m, ID2=20m, ID3=30m). Figures (b,e) show the influence of heave plates on the ID2 floater for the same draft of 20m. Figures (c,f) compare floaters of different dimensioning without heave plates for drafts of 10m (ID1 and 5) and 20m (ID 2,4).

With respect to heave, in the excitation load plots (Figure IV.7d-f), resonance around 0.6 rad/sec occurs. Increasing the draft (Figure IV.7d), the resonating frequency moves to the left and the excitation becomes sharper. When heave plates are added (Figure IV.7e) sharpens the excitation but does not affect the position of resonance. In this respect it is noted that resonance in this respect is exaggerated by linear theory and that in reality the waves within the torus will break. This does not suggest that these resonances can be

ignored. Then in Figure IV.7f comparisons among floaters of different size indicate that smaller inner diameters shift the resonating frequency to higher values.

Similar conclusions can be drawn from the RAOs, suggesting lower drafts and smaller inner diameters.

(a)

(d)

(b)

(e)

(c)

(f)

Figure IV.7 – RAOs (Left column) & Excitation Force plots (right column) in heave. Figures (a,d) show dependence on the draft (ID1=10m, ID2=20m, ID3=30m). Figures (b,e) show the influence of heave plates on the ID2 floater for the same draft of 20m. Figures (c,f) compare floaters of different dimensioning without heave plates for drafts of 10m (ID1 and 5) and 20m (ID 2,4).

(INNWIND.EU, Deliverable 4.3.3., Innovative Concepts for Floating Structures)

Conceptual conclusions and outlook

A torus shaped floater of the semi-submersible type (Concept 2) has been considered in various configurations. The draft was limited to 30 m in order to ensure suitability in a wide range of sea depths.

With respect to its hydrodynamic characteristics, it was shown that by tuning the draft and the inner diameter, the behaviour can be improved. For the cases considered, resonance in heave remained. Lower draft and smaller inner diameter indicated better behaviour which from an overall design perspective falls in the right direction. Smaller inner diameters favour the mounting of the wind turbine as indicated in Figure IV.3. Assuming that $H_b \sim 20\text{-}30$ m, the inclination of the supporting beams (or the tapering of a jacket like tower) would receive lower bending loads.

Also the costs when using concrete as indicated in Table IV.1 seem reasonable.

In further detailing this particular design, the dimensioning should undergo an optimization process. In this respect the corresponding cost function should include the cost of the floater as well as constraints regarding the loading on the wind turbine. To this end the ROM model reported in D 4.2.3 could be used in order to reduce the computational cost.

Finally the current stage for the particular floater concept can be classified as TRL 1.

(INNWIND.EU, Deliverable 4.3.3., Innovative Concepts for Floating Structures)

CONCLUSION

The conclusions were given at the end of each sub-chapter, i.e. conceptual description.

REFERENCES

[1] P. Chaviaropoulos, H. C. Karga and B. Hendriks, "InnWind.EU D1.2.3: PI-based Assessment of Innovative Concepts," 2014.

[2] S. Chakrabarti, Handbook of Offshore Engineering, Volume 1, Elsevier.

[3] S. Butterfield, J. Jonkman and P. P. Sclavounos, "Engineering Challenges for Floating Offshore Wind Turbines," 2007.

[4] P. Chaviaropoulos and A. Natarajan, "InnWind.EU D1.2.2: Definition of Performance Indicators (PIs) and Target Values," 2014.

[5] VDI, "VDI 2221 - Methodik zum Entwickeln und Konstruieren technischer Systeme und Produkte".

[6] J. Fernandez, A. Laidler, J. Izarra, M. Innovation, D. Murueta and B. Malloape, "Design considerations of a Semisubmersible Platform for Offshore Wind Turbines," in *Proceedings of the EWEA Offshore*, 2013.

[7] F. Huijs, J. Mikx, F. Savenije and E.-J. d. Ridder, "Integrated design of floater, mooring and control system for a semi-submersible floating wind turbine," *Proceedings of the EWEA Offshore,* 2014.

[8] S. Y. Hong, J. H. Kim, S. W. Hong and . H. J. Kim, "Design and Analysis of a Box Floater with Damping Plates for Floating Wind Turbine Platform," vol. 4, pp. 411-416, 2012.

[9] C. Molins, A. Campos, F. Sandner and D. Matha, "Monolithic Concrete Off-Shore Floating Structure For Wind Turbines," in *Proceedings of the EWEA*, 2014.

[10] K. Iijima, M. Kawai, Y. Nihei, M. Murai and T. Ikoma, "Conceptual Design Of A Single-Point-Moored Fowt And Tank Test For Its Motion Characteristics," 2013.

[11] R. W. Copple and C. Capanoglu, "Tension Leg Wind Turbine (TLWT) Conceptual Design Suitable for a Wide Range of Water Depths," vol. 4, pp. 396-403, 2012.

[12] K. Suzuki, H. Yamaguchi, M. Akase, A. Imakita, T. Ishihara, Y. Fukumoto and T. Oyama, "Initial Design of Tension Leg Platform for Offshore Wind Farm," *Journal of Fluid Science and Technology,* vol. 6, no. 3, pp. 372-381, 2011.

[13] C. Bak, F. Zahle, R. Bitsche, T. Kim, A. Yde, L. Henriksen, P. Andersen, A. Natarajan and M. Hansen, "Description of the DTU 10 MW Reference Wind Turbine," D1.21 INNWIND.EU, 2013.

[14] T. Fischer, W. de Vries and B. Schmidth, "Upwind Design Basis," 2010.

[15] A. Robertson, J. Jonkman, M. M, H. Song, A. Goupee, A. Coulling and C. Luan, "Definition of the Semisubmersible Floating System for Phase II of OC4," 2013.

[16] M. E. McCormick, Ocean Engineering Mechanics, Oxford University Press, 2010.

[17] DNV, "DNV-OS-J103 Design of Floating Wind Turbine Structures," 2013.

[18] A. Aubault, C. Cermelli and D. Roddier, "Parametric Optimization of a Semi-Submersible Platform With Heave Plates," in *Volume 1: Offshore Technology; Special Symposium on Ocean Measurements and Their Influence on Design*, 2007.

[19] T. I. Fossen, Handbook of Marine Craft Hydrodynamics and Motion Control, vol. First Edit, John Wiley & Sons, 2011.

[20] Ansys, *AQWA User Manual,* vol. 15317, 2011, pp. 724-746.

[21] Wamit, "Wamit User Manual 6.4".

[22] F. Sandner, D. Schlipf, D. Matha and P. W. Cheng, "Integrated Optimization Of Floating Wind Turbine Systems," in *Proceedings of the 33rd International Conference on Ocean, Offshore and Arctic Engineering OMAE*, San Francisco, 2014.

(INNWIND.EU, Deliverable 4.3.3., Innovative Concepts for Floating Structures)

[23] M. I. Kvittem, E. Bachynski and T. Moan, "Effects of Hydrodynamic Modelling in Fully Coupled Simulations of a Semi-submersible Wind Turbine," *Energy Procedia,* vol. 24, no. January, pp. 351-362, #jan# 2012.

[24] T. Burton, N. Jenkins, D. Sharpe and E. Bossanyi, Wind Energy Handbook, 2nd ed., Wiley, Ed., Wiley, 2011.

[25] D. Matha, "Model Development and Loads Analysis of an Offshore Wind Turbine on a Tension Leg Platform with a Comparison to Other Floating Turbine Concepts," 2009.

[26] M. Karimirad and T. Moan, "A Simplified Method for Coupled Analysis of Floating Offshore Wind Turbines," *Journal of Marine Structures,* vol. (Submitted, 2012.

[27] R. Lupton and R. Langley, "Efficient modelling of floating wind turbines," in *Proceedings of 9th PhD Seminar on Wind Energy in Europe*, Visby, 2013.

[28] G. Betti, M. Farina, G. Guagliardi, A. Marzorati and R. Scattolini, "Development and Validation of a Control-Oriented Model of Floating Wind Turbines," *IEEE Transactions on Control Systems Technology,* 2012.

[29] "INNWIND.EU Project Deliverable report 4.12," Aug. 2014.

[30] T. J. Larsen and A. M. Hansen, "How to HAWC2, the user's manual.," Tech. Rep. Risø-R-1597(ver.4-3) (EN), DTU Wind Energy, Roskilde, Denmark, May 2012.

[31] J.Jonkman, S.Butterfield, W.Musial and G. Scott, "Definition of a 5-MW Reference Wind Turbine for Offshore System Development," NREL Technical Report TP-500-38060, February, 2009.

[32] Norwegian Petroleum Directorate, "Norwegian Petroleum Directorate," Norwegian Petroleum Directorate, 2014. [Online]. Available: http://www.npd.no/en/. [Accessed 30 07 2014].

[33] A. Babarit, "NEMOH," Laboratoire de recherche en Hydrodynamique, Énergétique et Environnement Atmosphérique, [Online]. Available: http://lheea.ec-nantes.fr/doku.php/emo/nemoh/start. [Accessed 20 07 2014].

[34] F. Sandner and D. Matha, "Innovative Floating Platforms for Wind Turbines: Conceptual Design Stages," 10.Material cost estimation, pp.10, 4.07.2014.

[35] O. M. Faltinsen, "Sea loads on ships and offshore structures," Cambridge Ocean Technology Series.

[36] A. Robertson and J. Jonkman, "Definition of the Semisubmersible Floating System for Phase II of OC4".

[37] E. J. Azcona, "State-of-the-art and implementation of design tools for floating structures," INNWIND D4.21, 2013.

(INNWIND.EU, Deliverable 4.3.3., Innovative Concepts for Floating Structures)